# PIKfyve/Fab1 is required for efficient V-ATPase and hydrolase delivery to phagosomes, phagosomal killing, and restriction of *Legionella* infection

Catherine M. Buckley[1,2], Victoria L. Heath[3], Aurélie Guého[4], Cristina Bosmani[4], Paulina Knobloch[5], Phumzile Sikakana[1], Nicolas Personnic[5], Stephen K. Dove[6], Robert H. Michell[6], Roger Meier[7*], Hubert Hilbi[5], Thierry Soldati[4], Robert H. Insall[8#] and Jason S. King[1,2#]

[1]Centre for Membrane Interactions and Dynamics, Department of Biomedical Sciences, University of Sheffield, Firth Court, Western Bank, Sheffield. S10 2TN, UK

[2]Bateson Centre, University of Sheffield, Firth Court, Western Bank, Sheffield. S10 2TN, UK

[3]Institute of Cardiovascular Sciences, Institute for Biomedical Research, College of Medical and Dental Sciences, University of Birmingham, Edgbaston, Birmingham, B15 2TT, UK

[4]Department of Biochemistry, Faculty of Sciences, University of Geneva, CH-1211 Geneva, Switzerland

[5]Institute of Medical Microbiology, University of Zürich, CH-8006 Zürich, Switzerland

[6]School of Biosciences, University of Birmingham, Edgbaston, Birmingham. B15 2TT, UK

[7]Institute of Molecular Life Sciences, University of Zürich, CH-8057 Zürich, Switzerland

[8]CRUK Beatson Institute, Switchback Road, Bearsden, Glasgow G61 1BD, UK

[*]Present address: Scientific Center for Optical and Electron Microscopy, ETH Zürich, CH-8093 Zürich, Switzerland

[#]Address correspondence to Jason.King@sheffield.ac.uk, R.Insall@beatson.gla.ac.uk

**Running head:** PIKfyve in Dictyostelium

**Abstract word count:**

**Article word count:**

## Abstract

By engulfing potentially harmful microbes, professional phagocytes are continually at risk from intracellular pathogens. To avoid becoming infected, the host must kill pathogens in the phagosome before they can escape or establish a survival niche. Here, we analyse the role of the phosphoinositide (PI) 5-kinase PIKfyve in phagosome maturation and killing, using the amoeba and model phagocyte *Dictyostelium discoideum*.

PIKfyve plays important but poorly understood roles in vesicular trafficking by catalysing formation of the lipids phosphatidylinositol (3,5)-bisphosphate ($PI(3,5)_2$) and phosphatidylinositol-5-phosphate (PI(5)P). Here we show that its activity is essential during early phagosome maturation in *Dictyostelium*. Disruption of *PIKfyve* inhibited delivery of both the vacuolar V-ATPase and proteases, dramatically reducing the ability of cells to acidify newly formed phagosomes and digest their contents. Consequently, *PIKfyve*$^-$ cells were unable to generate an effective antimicrobial environment and efficiently kill captured bacteria. Moreover, we demonstrate that cells lacking *PIKfyve* are more susceptible to infection by the intracellular pathogen *Legionella pneumophila.* We conclude that PIKfyve-catalysed phosphoinositide production plays a crucial and general role in ensuring early phagosomal maturation, protecting host cells from diverse pathogenic microbes.

## Importance

Cells that capture or eat bacteria must swiftly kill them to prevent pathogens from surviving long enough to escape the bactericidal pathway and establish an infection. This is achieved by the rapid delivery of components that produce an antimicrobial environment in the phagosome, the compartment containing the captured microbe. This is essential both for the function of immune cells and for amoebae that feed on bacteria in their environment. Here we identify a central component of the pathway used by cells to deliver antimicrobial components to the phagosome and show that bacteria survive over three times as long within the host if this pathway is disabled. We show that this is of general importance for killing a wide range of pathogenic and non-pathogenic bacteria, and that it is physiologically important if cells are to avoid infection by the opportunistic human pathogen *Legionella*.

## Introduction

Professional phagocytes must kill their prey efficiently if they are to prevent the establishment of infections [1]. Multiple mechanisms are employed to achieve this. Once phagosomes have been internalised they quickly become acidified and acquire reactive oxygen species, antimicrobial peptides and acid hydrolases. The timely and regulated delivery of these components is vital to protect the host from intracellular pathogens but is incompletely understood.

After a particle is internalised, specific effector proteins are recruited to the phagosome's cytoplasmic surface by interacting with several inositol phospholipids (PIPs) that play important roles in regulating vesicle trafficking and controlling maturation. The effectors of each PIP regulate particular aspects of compartment identity, membrane trafficking and endosomal maturation [2, 3]. Phosphatidylinositol-3-phosphate (PI(3)P), made by the class III PI 3-kinase VPS34, is one of the first PIPs to accumulate on vesicles after endocytosis, and PI(3)P recruits proteins containing FYVE (Fab1, YOTB, Vac1 and EEA1) and PX domains, such as the canonical early endosome markers EEA1 and Hrs, and sorting nexins [4, 5]. Also recruited to early endosomes by its FYVE domain is PIKfyve (Fab1 in yeast) [6], a phosphoinositide 5-kinase that phosphorylates PI(3)P to phosphatidylinositol-3,5-bisphosphate (PI(3,5)$P_2$) [7-11]. The roles of PI(3)P are well explored but the formation of PI(3,5)$P_2$ and the identities and functions of its effector proteins and its metabolic product PI(5)P are less well understood [12-14]. PI(3,5)$P_2$ is thought to accumulate predominantly on late endosomes, and disruption of PIKfyve activity leads to multiple endocytic defects, including gross endosomal enlargement and accumulation of autophagosomes [15-20]. Recent research has begun to reveal important physiological roles of PIKfyve and its products in a variety of eukaryotes, but mechanistic details remain sparse [21-25].

As in classical endocytosis, phagosome maturation is regulated by PIPs [26]. Phagosomes accumulate PI(3)P immediately after closure, and this is required for their subsequent maturation [27-29]. The recent identification of several PIKfyve inhibitors, including apilimod and YM201636 [30, 31], has allowed researchers to demonstrate the importance of PI(3)P to PI(3,5)$P_2$ conversion for phagosomal maturation in macrophages and neutrophils [32-35]. However, there are conflicting reports on the roles of PIKfyve in key lysosomal functions such as acidification and degradation, with some studies reporting defective acidification upon PIKfyve inhibition [10, 36, 37] and others finding little effect [33, 38, 39]. Therefore the mechanistic roles of PIKfyve and its products, and their relevance to phagosome maturation, remain unclear and subject to debate.

To understand the function and physiological significance of PIKfyve, we have investigated its role in phagosome maturation and pathogen killing in *Dictyostelium discoideum,* a soil-dwelling amoeba

84 and professional phagocyte that feeds on bacteria. *Dictyostelium* PIPs are unusual, with the lipid
85 chain joined to the *sn*-1-position of the glycerol backbone by an ether, rather than ester, linkage:
86 these PIPs should correctly be named as derivatives of plasmanylinositol rather than
87 phosphatidylinositol [40]. This, however, makes no known difference to downstream functions,
88 which are dictated by interactions between the inositol polyphosphate headgroups and effector
89 proteins. *Dictyostelium* has thus been an effective model for analysis of phosphoinositide signalling
90 [41-44]. For convenience, both the mammalian and *Dictyostelium* inositol phospholipids are referred
91 to as PIPs hereafter.

92 We find that genetic or pharmacological disruption of PIKfyve activity in *Dictyostelium* leads to a
93 swollen endosomal phenotype reminiscent of defects in macrophages. We provide a detailed
94 analysis of phagosome maturation, and show that at least some of the defects in PIKfyve-deficient
95 cells are due to reduced recruitment of the proton-pumping vacuolar (V-ATPase). Finally, we
96 demonstrate that PIKfyve activity is required for the efficient killing of phagocytosed bacteria and for
97 restricting the intracellular growth of the pathogen *Legionella pneumophila.*

98

99 ## Results

100 ***PIKfyve⁻ Dictyostelium* have swollen endosomes**

101 The *Dictyostelium* genome contains a single orthologue of *PIKfyve* (*PIP5K3*). Like the mammalian and
102 yeast proteins, *Dictyostelium* PIKfyve contains an N-terminal FYVE domain, a CCT (chaperonin
103 Cpn60/TCP1)-like chaperone domain, a PIKfyve-unique cysteine/histidine-rich domain and a C-
104 terminal PIP kinase domain [7]. In order to investigate the role of PI(3,5)$P_2$ in *Dictyostelium* we
105 disrupted the *PIKfyve* gene in the axenic Ax3 background by inserting a blasticidin resistance cassette
106 and deleting a portion of the central PIKfyve-unique region (Supplementary Figure 1).

107 While the unusual ether-linked chemistry of the *Dictyostelium* inositol phospholipids prevented
108 direct measurement of PI(3,5)$P_2$ loss by either the standard method of methanolysis followed by
109 HPLC of deacylation products or by mass spectrometry, we found that each mutant strain was highly
110 vacuolated (Figure 1A and B), resembling the swollen vesicle phenotype observed upon *PIKfyve*
111 knockdown or inhibition in mammalian cells, *C. elegans*, *S. cerevisiae* and *D. melanogaster* [10, 15,
112 20, 45]. This effect was recapitulated by incubation with the PIKfyve-specific inhibitor apilimod [30],
113 confirming that this phenotype was due to deficient PIKfyve activity, most likely via the production
114 of PI(3,5)$P_2$ or PI(5)P (Figure 1C).

115 When *PIKfyve*- amoebae were hypotonically stressed in phosphate buffer, we observed a sustained
116 increase in vacuolation for at least 5 hours. However, after 24 hours – when the cells became
117 polarized indicating the onset of starvation-induced development – *PIKfyve*- mutants became
118 indistinguishable from the random integrant and parental controls (Figure 1B). This is most likely due
119 to the suppression of fluid-phase uptake that occurs when *Dictyostelium* cells enter starvation-
120 induced development [46, 47]. Consistent with this interpretation, *PIKfyve⁻* cells had no observable
121 delay or other defects in development, and formed morphologically normal fruiting bodies with
122 viable spores (Supplementary Figure 2). Therefore, disruption of PIKfyve leads to endocytic defects
123 but it is not required for *Dictyostelium* development.

124 **PIKfyve is important for phagocytic growth but not uptake**

125 Laboratory strains of *Dictyostelium* can obtain nutrients by macropinocytosis of liquid (axenic)
126 medium or by phagocytosis of bacteria. Whilst *PIKfyve⁻* cells had normal rates of both endocytosis
127 and exocytosis, axenic growth was slower than for wild-type cells, with mutants doubling every 16
128 hours compared to 10 hours for the controls (Figure 2A-C).

129 Growth on bacteria was more strongly affected. When we measured phagocytosis by following the
130 ability of *Dictyostelium* cells to decrease the turbidity of an *E. coli* suspension over time we found no

131 significant defects in *PIKfyve*$^-$ cells (Figure 2D). In contrast, they grew significantly more slowly on a
132 lawn of *Klebsiella pneumoniae* (Figure 2E). This indicates a specific role for PIKfyve activity in
133 phagosome maturation rather than bacterial uptake.

134 ***PIKfyve* deficient cells have defective phagosome acidification and V-ATPase delivery**

135 Next we investigated how the absence of PIKfyve affects phagosomal maturation. One of the first
136 stages of maturation is the acquisition of the proton-pumping V-ATPase, leading to rapid
137 acidification [48, 49]. The influence of PIKfyve on endosomal pH regulation remains controversial:
138 studies in *C. elegans,* plants, and mammalian epithelial cells have shown that PIKfyve is required for
139 efficient acidification [37, 45, 50-52], but RAW 264.7 macrophages are still able to acidify their
140 phagosomes to at least pH 5.5 when treated with a PIKfyve inhibitor [33].

141 Phagosome maturation is well characterised in *Dictyostelium,* with most studies being performed
142 using mutants in the Ax2 genetic background, rather than Ax3 as used above. For comparison with
143 other studies we isolated additional mutants from Ax2 cells, which were used for all subsequent
144 experiments unless stated otherwise. Ax2 background *PIKfyve* mutants also exhibited slow growth
145 on bacterial lawns but normal phagocytosis of both beads and bacteria (supplementary figure 3),
146 confirming that these phenotypes are robust across multiple genetic backgrounds.

147 We followed phagosome acidification in *PIKfyve*$^-$ *Dictyostelium* by measuring changes in the relative
148 fluorescence of engulfed beads that had been labelled both with the pH-sensitive FITC and the pH-
149 insensitive Alexa 594 succinimidyl ester [53]. Phagosomes from wild-type cells rapidly became
150 acidified and remained acidic until ~40 minutes before transitioning to neutral post-lysosomes, but
151 phagosomes of *PIKfyve*$^-$ cells acidified much more slowly and never achieved as low a pH (Figure 3A).

152 Phagosomal acidification is driven by the rapid recruitment and activity of the V-ATPase. To
153 differentiate between defective V-ATPase delivery and activity, we directly imaged recruitment of
154 the VatM transmembrane subunit of the V-ATPase fused to GFP to nascent phagosomes by
155 microscopy. By observing the phagocytosis of pH-sensitive pHrodo-labelled yeast we were able to
156 simultaneously monitor acidification.

157 GFP-VatM began accumulating on phagosomes immediately following internalisation both in
158 *PIKfyve*$^-$ and control cells, but it accumulated more slowly in the mutants and to only about half of
159 the levels observed in wild-type cells (Figure 3B and C). Defective acidification was further
160 demonstrated by a reduced increase in pHrodo fluorescence (Figure 3D). We conclude that there is
161 some PIKfyve-independent lysosomal fusion with phagosomes, but that PIKfyve activity is required
162 for the high levels of V-ATPase accumulation that are needed for efficient phagosomal acidification.

163 The V-ATPase consists of $V_0$ (transmembrane) and $V_1$ (peripheral) subcomplexes. It has previously
164 been suggested that PI(3,5)$P_2$ can regulate $V_0$-$V_1$ assembly at the yeast vacuole allowing dynamic
165 regulation of activity [54]. VatM is a component of the $V_0$ subcomplex (subunit a in mammals and
166 yeast). To test whether $V_0$-$V_1$ association is also affected by loss of PIKfyve we observed the
167 phagosomal recruitment of the $V_1$ subunit VatB fused to GFP [55]. Both GFP-VatM and VatB-GFP
168 were expressed equally in wild-type and mutant cells (Supplementary Figure 4A). As before VatB-
169 GFP recruitment to nascent phagosomes was also significantly decreased in *PIKfyve*- cells
170 (Supplementary Figure 4B and C)

171 It should be noted that expression of VatB-GFP (but not GFP-VatM) caused a partial inhibition of
172 acidification in this assay, indicating caution should be taken in using this construct (Supplementary
173 Figure 4D). Nevertheless, the observation that both V-ATPase components were equally affected by
174 PIKfyve deletion suggests that PIKfyve is required for delivery of the entire V-ATPase to the
175 phagosome, rather than specifically affecting $V_0$-$V_1$ association.

176 **Proteolytic activity and hydrolase delivery are specifically affected in *PIKfyve*$^-$ cells**

177 Proper degradation of internalised material requires both acidification and the activity of proteases.
178 To test if hydrolytic activity was also dependent on PIKfyve, we measured phagosomal proteolysis by
179 following the increase in fluorescence due to the cleavage and unquenching of DQ-bovine serum
180 albumin (DQ-BSA) coupled to beads [53] (Figure 4A). Strikingly, despite their partial acidification,
181 phagosomes in *PIKfyve*$^-$ cells exhibited an almost complete loss of proteolytic activity. To control for
182 a potential general decrease in protease activity, we measured the unquenching of DQ-BSA beads in
183 whole cell lysates (Figure 4B) and the protein levels of lysosomal protease cathepsin D by Western
184 blot (Figure 4C and D). Although activity in the phagosome is completely lost, we found that total
185 lysosomal activity remained normal and cathepsin D levels were significantly increased upon loss of
186 *PIKfyve*, consistent with a defect in delivery to the phagosome, rather than in lysosomal biogenesis.

187 To investigate whether PIKfyve activity was required to deliver proteases to the phagosome, we
188 purified phagosomes at different stages of maturation and analysed their composition by Western
189 blot (Figure 4E). In wild-type cells phagosomes acquired cathepsin D from the earliest time-point,
190 but the protease was almost completely absent from phagosomes in *PIKfyve*- cells. Whilst the
191 delivery of the vacuolar ATPase was also qualitatively reduced in this assay, consistent with
192 decreased acidification, Actin-binding protein 1 (Abp1), an independent marker of phagosome
193 maturation [56], was unaffected. Thus, although both hydrolase and to a lesser extent V-ATPase
194 delivery requires PIKfyve activity, other aspects of maturation appear to progress normally.

195 **PIKfyve does not regulate PI(3)P dynamics**

196 We next wanted to confirm whether loss of PIKfyve disrupts specific aspects of phagosome
197 maturation or causes a general trafficking defect. PI(3)P is one of the best characterized early
198 markers of maturing endosomes and phagosomes in both mammalian macrophages and
199 *Dictyostelium.* Immediately following particle internalization, PI(3)P is generated on the phagosome
200 by the class III PI 3-kinase VPS34 [27, 33, 57] and interacts with a number of important regulators of
201 maturation such as Rab5 [58]. PIKfyve is both recruited by PI(3)P and phosphorylates it, forming
202 PI(3,5)$P_2$. Loss of PIKfyve activity could perturb phagosome maturation by reducing PI(3)P
203 consumption, by eliminating the actions of PI(3,5)$P_2$, or both. Studies on macrophages have
204 indicated that inhibition of PIKfyve can cause prolonged PI(3)P signalling [33].

205 PI(3)P can be visualized in cells using the well-characterised reporter GFP-2xFYVE [41, 59].
206 Expression of GFP-2xFYVE in control cells demonstrated that PI(3)P is present on *Dictyostelium*
207 phagosomes immediately following engulfment, consistent with previous reports [57] (Figure 4F).
208 However, we found no abnormalities in either the recruitment to or the dissociation from
209 phagosomes of this reporter in *PIKfyve*- mutants (Figure 4F and G). PIKfyve activity seems not to
210 influence the steady-state levels of PI(3)P in *Dictyostelium*, and the functional defects in *PIKfyve*-
211 cells therefore are likely to be caused by a lack of the product(s) of PIKfyve activity.

212 Overall, the normal transition of *PIKfyve*- phagosomes into a PI(3)P-negative compartment indicates
213 that much of their phagosome maturation process continues normally – but with the product(s) of
214 PIKfyve action playing specific role(s) in the delivery of certain important components, including the
215 V-ATPase and hydrolytic enzymes.

216 **PIKfyve is essential for efficient killing of bacteria**

217 Acidification and proteolysis are important mechanisms used by phagocytes to kill engulfed
218 microbes. We therefore asked whether PIKfyve was physiologically important for killing. Bacterial
219 death leads to membrane permeabilisation and intracellular acidification, so survival time within
220 phagosomes can be inferred by observing the phagocytosis and subsequent quenching of GFP
221 fluorescence when expressed by a non-pathogenic *Klebsiella pneumoniae* strain [60]. In this assay,
222 the phagocytosed bacteria survived more than three times longer in *PIKfyve*$^-$ cells (median survival
223 12 min) than in wild-type cells (3.5 min) (Figure 5A and B). These benign bacteria did eventually die
224 in *PIKfyve*$^-$ cells, indicating either that the residual acidification is eventually sufficient or that enough
225 other elements of the complex bacterial killing machinery remain functional in *PIKfyve*$^-$ phagosomes.

226 These defects in bacterial killing and digestion (Figure 4) explain why PIKfyve is important for
227 *Dictyostelium* to grow on a lawn of *K. pneumoniae* (Figure 2E). To test whether this is general to a
228 broad range of bacteria, we employed an assay whereby serial dilutions of amoebae are plated on
229 lawns of a panel including both Gram-positive and Gram-negative bacteria [61]. In this assay,
230 *PIKfyve*-deficient cells were severely inhibited in growth on all bacteria tested, demonstrating a
231 general role for PIKfyve in bacterial killing and digestion.

232 **PIKfyve activity restricts the persistence of *Legionella* infection**

233 Many pathogenic bacteria infect host immune cells by manipulating phagosome maturation to
234 establish a replication-permissive niche or to escape into the cytosol. To avoid infection, host cells
235 must efficiently kill such pathogens; hence PIKfyve might be critical to protect host cells from
236 infection.

237 *Legionella pneumophila* is a Gram-negative opportunistic human pathogen that normally lives in the
238 environment by establishing replicative niches inside amoebae such as *Acanthamoeba.* This process
239 can be replicated in the laboratory using *Dictyostelium* as an experimental host [62]. Following its
240 phagocytosis, *Legionella* can disrupt normal phagosomal maturation and form a unique *Legionella*-
241 containing vacuole (LCV). This requires the Icm/Dot (Intracellular multiplication/Defective for
242 organelle trafficking) type IV secretion system that delivers a large number of bacterial effector
243 proteins into the host (reviewed in [63]). These effectors modify many host signalling and trafficking
244 pathways, one of which prevents the nascent *Legionella*-containing phagosome from fusing with
245 lysosomes [64].

246 Phosphoinositide signalling is heavily implicated in *Legionella* pathogenesis, with *Legionella*-
247 containing phagosomes rapidly accumulating PI(3)P. Its concentration then declines within 2 hours
248 and PI(4)P accumulates [65]. Multiple effectors introduced through the Icm/Dot system bind PI(3)P
249 or PI(4)P [66-72]. The role of PI(3,5)$P_2$ (and/or PI(5)P) in *Legionella* infection is yet to be investigated,
250 so we tested whether PIKfyve was beneficial or detrimental for the host to restrain *Legionella*
251 infection.

252 When we measured the rate of uptake of GFP-expressing *Legionella* by flow cytometry, we found
253 *PIKfyve*$^-$ *Dictyostelium* were indistinguishable from wild-type. Both strains phagocytosed many more
254 of the virulent wild-type *Legionella* strain (JR32) than an avirulent strain that is defective in type IV
255 secretion (*ΔicmT*) [73] (Figure 6A). These results are in agreement with the previous finding that
256 expression of the Icm/Dot T4SS promotes uptake of *Legionella* [74]. When we measured the ability

257 of *Dictyostelium* to kill *Legionella ΔicmT,* the bacteria survived for significantly longer in *PIKfyve*- cells
258 (Figure 6B).

259 We next tested the role of PIKfyve on the outcome of infection. When Ax2 and PIKfyve mutants
260 were infected with either wild-type or *ΔicmT Legionella,* using a MOI of 0.1 to compensate for the
261 greater uptake of wild-type *Legionella*, both amoeba strains suppressed the avirulent bacteria,
262 although the reduction in bacteria was slower in the *PIKfyve* mutants. In contrast, wild-type
263 *Legionella* grew substantially faster in cells lacking PIKfyve (Figure 6C, note that the CFUs scales in
264 Figure 6B and C are logarithmic). We independently confirmed these results using flow cytometry of
265 cells infected with GFP-producing bacteria in our Ax3-background mutants. The only *Dictyostelium*
266 cells that accumulated substantial GFP fluorescence over several days were those infected by wild-
267 type *Legionella*, and this happened sooner and to a greater degree in the *PIKfyve*- cells (Figure 6D).

268 Unlike PI(3)P and PI(4)P, the lipid products of PIKfyve are thus not required for *Legionella* to subvert
269 phagosome maturation and generate its replicative vacuole. Rather, the role of PIKfyve in ensuring
270 rapid phagosomal acidification and digestion is crucial for the host to prevent *Legionella*, and
271 presumably other pathogens, from surviving and establishing a permissive niche.

272

## Discussion

In this study, we have characterised the role of PIKfyve during phagosome maturation using the model phagocyte *Dictyostelium.* The roles of PI 3-kinases and PI(3)P signalling during phagosome formation and early maturation have been studied extensively but the subsequent actions of PIKfyve and roles of PI(3,5)$P_2$ and PI(5)P are much less well understood [3, 26]. In non-phagocytic cells such as fibroblasts and yeast, PI(3,5)$P_2$ production is important for endosomal fission and fragmentation of endolysosomal compartments [10, 18, 37, 45], and PIKfyve inhibition has been shown to cause macrophage lysosomes to coalesce by an unknown mechanism [34]. PIKfyve also regulates macropinosome maturation [38], intracellular replication of the *Vaccinia* virus and *Salmonella* [38, 51, 75] and production of reactive oxygen species (ROS) in neutrophils [35]. In this paper we show that PIKfyve is critical to ensure efficient phagosomal acidification and proteolysis via delivery of specific components, and we demonstrate its physiological importance in the killing of bacteria and suppression of intracellular pathogens.

Complex effects of PIKfyve inhibition on PIP-mediated signalling have hampered clear interpretation of PIKfyve function in some mammalian studies. For example, some studies report that disruption of PIKfyve both prolonged PI(3)P-mediated signalling and eliminated PI(3,5)$P_2$ production [30, 32], making it difficult to determine which phosphoinositide change is responsible for the observed phenotypes. In contrast, and in agreement with other reports in mammalian cells [18, 37], we found that deletion of PIKfyve had no impact on phagosomal PI(3)P dynamics in *Dictyostelium*. The defects in phagosome maturation that we observed in this system are thus due to lack of PI(3,5)$P_2$/PI(5)P formation and not to prolonged PI(3)P signalling. There is limited evidence that PIKfyve might exhibit protein kinase activity [76], but whether this is relevant *in vivo* remains to be shown.

The role of PIKfyve in lysosomal acidification and degradation is currently disputed. Several studies which have measured vesicular pH at a single time point have shown that PIKfyve is required for acidification [10, 37, 45, 52], whereas others found that disruption of PIKfyve had little effect on phagosomal pH [33, 38, 39]. In contrast, we followed the temporal dynamics of V-ATPase delivery and of phagosomal acidification and proteolysis, and showed that V-ATPase delivery to PIKfyve-deficient phagosomes was substantially decreased and delayed, with consequent defects on initial acidification and proteolysis. PI(3,5)$P_2$ has also been proposed to regulate V-ATPase $V_0$-$V_1$ subcomplex association dynamically at the yeast vacuole [54], but we found no evidence for this during *Dictyostelium* phagosome maturation.

It is still not clear how PIKfyve-generated PI(3,5)$P_2$ regulates V-ATPase trafficking, and few PI(3,5)$P_2$ effectors are known. One of these is the lysosomal cation channel TRPML1/mucolipin, which is

306 specifically activated by PI(3,5)$P_2$ [77]. This interaction was recently shown to partly underlie the role
307 of PIKfyve in macropinosome fragmentation, although not acidification [38]. TRPML1 is also required
308 for phagosome-lysosome fusion [78], and PI(3,5)$P_2$ and TRPML1 have been proposed to mediate
309 interactions between lysosomes and microtubules [79]. PIKfyve may therefore drive V-ATPase
310 delivery to phagosomes both by microtubule-directed trafficking and by regulating fission. However,
311 the sole mucolipin orthologue in *Dictyostelium* is only recruited to phagosomes much later, during
312 the post-lysosomal phase, and its disruption influences exocytosis rather than acidification [80].

313 Effective phagosomal acidification and proteolysis is essential if phagocytes are to kill internalised
314 bacteria. Many clinically relevant opportunistic pathogens, including *Legionella* [63, 81],
315 *Burkholderia cenocepacia* [82] and *Cryptococcus neoformans* [83], have developed the ability to
316 subvert normal phagosome maturation so as to maintain a permissive niche inside host phagocytes.
317 This ability is likely to have evolved from their ancestors' interactions with environmental predators
318 such as amoebae [84-86].

319 *Legionella* are phagocytosed in the lung by alveolar macrophages. After internalisation, they employ
320 effectors secreted via their Type IV secretion system, some of which interfere with PI(3)P-signalling,
321 to inhibit phagosome maturation [67, 87, 88]. We have shown that the products of PIKfyve are not
322 required for *Legionella* to establish an intracellular replication niche. Rather, *Legionella* survive much
323 better in PIKfyve-deficient cells, suggesting that PI(3,5)$P_2$ helps *Dictyostelium* to eliminate rather
324 than harbour *Legionella*.

325 This is in contrast to the non-phagocytic invasion of epithelia that occurs during *Salmonella* infection.
326 In that case, PIKfyve activity is necessary to promote the generation of a specialised survival niche
327 within which the bacteria replicate [51]. *Salmonella* has thus evolved a specific requirement for
328 PIKfyve in generating a survival niche – likely through using phagosome acidification as a cue for
329 virulence factor expression – whereas *Legionella* and other bacteria are suppressed by rapid and
330 PIKfyve-driven phagosomal maturation.

331 The molecular arms race between host and pathogens is complex and of great importance. The very
332 early events of phagosome maturation are critical in this competition; host cells aim to kill their prey
333 swiftly whilst pathogens try to survive long enough to escape. Although its molecular effectors
334 remain unclear, PIKfyve and its products are crucial to tip the balance in favour of the host, providing
335 a general mechanism to ensure efficient antimicrobial activity.

336 ## Materials and Methods

337 ### Cell strains and culture

338 *Dictyostelium discoideum* cells were grown in adherent culture in plastic Petri dishes in HL5 medium
339 (Formedium) at 22°C. *PIKfyve*$^-$ mutants were generated in both Ax2 and Ax3 backgrounds, with
340 appropriate wild-type controls used in each case. Cells were transformed by electroporation and
341 transformants selected in 20 µg/ml hygromycin (Invitrogen) or 10 µg/ml G418 (Sigma). Apilimod was
342 from United States Biological.

343 Growth in liquid culture was measured by seeding log phase cells in a 6 well plate and counting cells
344 every 12 hours using a haemocytometer. Growth on bacteria was determined by plating ~10
345 *Dictyostelium* cells on SM agar plates (Formedium) spread with a lawn of non-pathogenic KpGe *K.*
346 *pneumoniae* [89].

347 Plaque assays were performed as previously described [90]. Briefly, serial dilution of *Dictyostelium*
348 cells (10-$10^4$) were placed on bacterial lawns and grown until visible colonies were obtained. The
349 bacterial strains were kindly provided by Pierre Cosson and were: *K. pneumoniae* laboratory strain
350 and 52145 isogenic mutant (Benghezal et al., 2006), the isogenic *P. aeruginosa* strains PT5 and
351 PT531 (*rhlR-lasR* avirulent mutant) (Cosson et al., 2002), *E.coli* DH5α (Fisher Scientific), *E. coli* B/r
352 (Gerisch, 1959), non-sporulating *B. subtilis* 36.1 (Ratner and Newell, 1978), and *M. luteus*
353 (Wilczynska and Fisher, 1994). An avirulent strain of *K. pneumoniae* was obtained from ATCC (Strain
354 no. 51697).

355 The *Dictyostelium* development was performed by spreading $10^7$ amoebae on nitrocellulose filters
356 (47 mm Millipore) on top of absorbent discs pre-soaked in KK2 (0.1 M potassium phosphate pH 6.1)
357 and images were taken at 20 hours [91].

358 ### Gene disruption and molecular biology

359 *PIKfyve*$^-$ cells in an Ax2 background were generated by gene disruption using homologous
360 recombination. A blasticidin knockout cassette was made by amplifying a 5' flanking sequence of the
361 *PIKfyve* gene (DDB_G0279149) (primers: fw- GGTAGATGTTTAGGTGGTGAAGT, rv-
362 gatagctctgcctactgaagCGAGTGGTGGAATTCATAAAGG) and 3' flanking sequence (primers: fw-
363 ctactggagtatccaagctgCCATTCAAGATAGACCAACCAATAG, rv- AGAATCAGAATAAACATCACCACC). These
364 primers contained cross over sequences (in lower case) allowing a LoxP-flanked blasticidin resistance
365 cassette (from pDM1079, a kind gift from Douwe Veltman) to be inserted between the two arms.

366 For *PIKfyve* gene disruption in an Ax3 background a knockout cassette was constructed in
367 pBluescript by sequentially cloning fragment I (amplified by

368 TAGTAGGAGCTCGGATCCGGTAGATGTTTAGGTGGTGAAGTTTTACCAAC and
369 TAGTAGTCTAGACGAGTGGTGGAATTCATAAAGGTACGTTCAT) and fragment II (amplified by
370 TAGTAGAAGCTTCCATTCAAGATAGACCAACCAATAGTAGTCCTGC and
371 TAGTAGGGTACCGGATCCCAGTGTGTAAATGAGAATCAGAATAAACATCACC). The blasticidin resistance
372 gene was inserted between fragment I and II as an XbaI – HindIII fragment derived from pBSRδBam
373 [92]. Both constructs were linearised, electroporated into cells and colonies were screened by PCR.
374 GFP-2xFYVE was expressed using pJSK489 [41] and GFP-$PH_{CRAC}$ with pDM631 [93]. VatM and VatB
375 were cloned previously [94] but subcloned into the GFP-fusion expression vectors pDM352 and 353
376 [95] to give plasmids pMJC25 and pMJC31 respectively.

377 ## Microscopy and image analysis

378 Fluorescence microscopy was performed on a Perkin-Elmer Ultraview VoX spinning disk confocal
379 microscope running on an Olympus 1x81 body with an UplanSApo 60x oil immersion objective (NA
380 1.4). Images were captured on a Hamamatsu C9100-50 EM-CCD camera using Volocity software by
381 illuminating cells with 488 nm and 594 nm laser lines. Quantification was performed using Image J
382 (https://imagej.nih.gov).

383 To image PI(3)P dynamics, cells were incubated in HL5 medium at 4 °C for 5 mins before addition of
384 10 µl of washed 3 µm latex beads (Sigma) and centrifugation at 280 x *g* for 10 seconds in glass-
385 bottomed dishes (Mat-Tek). Dishes were removed from ice and incubated at room temperature for
386 5 mins before imaging. Images were taken every 30 s across 3 fields of view for up to 30 mins.

387 V-ATPase recruitment and acidification was performed using *Saccharomyces cerevisiae* labelled with
388 pHrodo red (Life Technologies) as per the manufacturers instructions. *Dictyostelium* cells in HL5
389 medium were incubated with $1x10^7$ yeast per 3 cm dish, and allowed to settle for 10 mins before the
390 medium was removed and cells were gently compressed under a 1% agarose/HL5 disk. Images were
391 taken every 10 s across 3 fields of view for up to 20 mins. Yeast particles were identified using the
392 "analyse particles" plugin and mean fluorescence measured over time. V-ATPase recruitment was
393 measured as the mean fluorescence within a 0.5 µm wide ring selection around the yeast. The signal
394 was then normalised to the initial fluorescence after yeast internalisation for each cell.

395 ## Endocytosis and exocytosis

396 To measure endocytosis, *Dictyostelium* at $5 \times 10^6$ cells/ml were shaken at 180 rpm for 15 mins in HL5
397 before addition of 100 mg/ml FITC dextran (molecular mass, 70 kDa; Sigma). At each time point 500
398 µl of cell suspension were added to 1 ml ice-cold KK2 on ice. Cells were pelleted at 800 x *g* for 2 mins
399 and washed once in KK2. The pellet was lysed in 50 mM $Na_2HPO_4$ pH 9.3 0.2% Triton X-100 and

400 measured in a fluorimeter. To measure exocytosis, cells were prepared as above and incubated in 2
401 mg/ml FITC-dextran overnight. Cells were pelleted, washed twice in HL5 and resuspended in HL5 at 5
402 × $10^6$ cells/ml. 500 µl of cell suspension were taken for each time point and treated as described
403 above.

## 404 Phagocytosis and phagosomal activity assays

405 Phagocytosis of *E. coli* was monitored by the decrease in turbidity of the bacterial suspension over
406 time as described [96]. An equal volume of 2 × $10^7$ *Dictyostelium* cells was added to a bacterial
407 suspension with an $OD_{600\,nm}$ of 0.8, shaking at 180 rpm, and the decrease in $OD_{600\,nm}$ was recorded
408 over time. Phagocytosis of GFP-expressing *M. smegmatis* and 1 µm YG-carboxylated polystyrene
409 beads (Polysciences Inc.) was previously described [53, 97]. 2 × $10^6$ *Dictyostelium*/ml were shaken for
410 2 hours at 150 rpm. Either 1 µm beads (at a ratio of 200:1) or *M. smegmatis* (multiplicity of infection
411 (MOI) 100) were added, 500 µl aliquots of cells were taken at each time point and fluorescence was
412 measured by flow cytometry [53].

413 Phagosomal pH and proteolytic activity were measured by feeding cells either FITC/TRITC or
414 DQgreen- BSA/Alexa 594-labelled 3 µm silica beads (Kisker Biotech) [53]. Briefly, cells were seeded in
415 a 96 well plate before addition of beads and fluorescence measured on a plate reader over time. pH
416 values were determined by the ratio of FITC to TRITC fluorescence using a calibration curve and
417 relative proteolysis was normalised to Alexa594 fluorescence. To measure proteolytic activity in cell
418 lysates 4 x $10^7$ cells/ml were resuspended in 150 mM potassium acetate pH 4.0 and lysed by 3 cycles
419 of freeze/thaw in liquid nitrogen. After pelleting cell debris at 15000 rpm for 5 minutes at 4°C, 100 µl
420 of lysate was added per well. Proteolytic activity was measured on a plate reader in triplicate, as
421 described above, using 1 x $10^8$ DQ-BSA/Alexa594 beads per cell. A 5 x final concentration of HALT
422 protease inhibitor cocktail (Life Technologies) was added to samples as a negative control.

## 423 Phagosome isolation and blotting

424 *Dictyostelium* phagosomes were purified at different stages in maturation after engulfment of latex
425 beads as previously described [98]. Briefly $10^9$ cells per timepoint were incubated with a 200-fold
426 excess of 0.8 µm diameter beads (Sigma) first in 5 ml ice-cold Soerensen buffer containing 120 mM
427 sorbitol (SSB) pH 8 for 5 minutes, then added to 100 ml room-temperature HL5 medium in shaking
428 culture (120 rpm) for 5 (first time point) or 15 minutes to allow phagocytosis (pulse). Engulfment
429 was stopped by adding cells to 300ml ice-cold SSB and centrifugation. After washing away non-
430 engulfed beads, cells were again shaken in room-temperature HL5 for the times indicated (chase) to
431 allow maturation. At each time point, maturation was stopped using ice-cold SSB as above, and cells
432 pelleted. Phagosomes were purified as in [56], after homogenization using 10-passages through a

433 ball homogeniser (void clearance 10 µm). The homogenate was incubated with 10 mM Mg-ATP
434 (Sigma) for 15 minutes before loading onto a discontinuous sucrose gradient. Phagosomes were
435 collected from the 10-25% interface, normalised by light scattering at 600 nm and analysed by
436 Western blot. Antibodies used were anti-VatA mAB 221-35-2 (gift from G. Gerisch), anti-vatM mAb
437 N2 [99]; rabbit anti-cathepsin D [100] and anti-Abp1 [101]. All blots were processed in parallel from
438 the same lysates with identical exposure and processing between cell lines.

439 ## Bacteria killing assay

440 Killing of GFP-expressing *K. pneumoniae* was measured as previously described [60]. Briefly, 10 µl of
441 an overnight culture of bacteria in 280 µl HL5 was placed in a glass-bottomed dish and allowed to
442 settle before careful addition of 1.5 ml of a *Dictyostelium* cell suspension at $1 \times 10^6$ cells/ml. Images
443 were taken every 20 s for 40 min at 20x magnification. Survival time was determined by how long
444 the GFP-fluorescence persisted after phagocytosis.

445 ## Western blotting

446 Ax2 or *PIKfyve*$^-$ cells expressing GFP-VatM or VatB-GFP were analysed by SDS-PAGE and Western blot
447 using a rabbit anti-GFP primary antibody (gift from A. Peden) and a fluorescently conjugated anti-
448 rabbit 800 secondary antibody, using standard techniques. The endogenous biotinylated
449 mitochondrial protein Methylcrotonoyl-CoA Carboxylase 1 (MCCC1) was used as a loading control
450 using Alexa680-conjugated Streptavadin (Life Technologies) [102].

451 ## *Legionella* infection assays

452 The following *L. pneumophila* Philadelphia-1 strains were used: virulent JR32 [103], the isogenic
453 Δ*icmT* deletion mutant GS3011 lacking a functional Icm/Dot type IV secretion system [73], and
454 corresponding strains constitutively producing GFP [74]. *L. pneumophila* was grown for 3 days on
455 charcoal yeast extract (CYE) agar plates, buffered with *N*-(2-acetamido)-2-aminoethane-sulfonic acid
456 (ACES) [104]. For infections, liquid cultures were inoculated in AYE medium at an $OD_{600}$ of 0.1 and
457 grown for 21 h at 37 °C (post-exponential growth phase). To maintain plasmids, chloramphenicol
458 was added at 5 µg/ml.

459 Uptake by *D. discoideum*, intracellular replication or killing of GFP-producing *L. pneumophila* was
460 analyzed by flow cytometry as described [71]. Exponentially growing amoebae were seeded onto a
461 24-well plate ($1 \times 10^6$ cells/ml HL5 medium per well) and allowed to adhere for at least 1–2 h. *L.*
462 *pneumophila* grown for 21 h in AYE medium was diluted in HL5 medium and used to infect the
463 amoebae at an MOI of 50. The infection was synchronized by centrifugation (10 min, 500 x *g*), and
464 infected cells were incubated at 25 °C for 30 min before extracellular bacteria were removed by

465 washing twice with SorC (2 mM $Na_2HPO_4$, 15 mM $KH_2PO_4$, 50 µM $CaCl_2$, pH 6.0). Infected amoebae
466 were detached by vigorously pipetting and fixed (PFA 2%, sucrose 125 mM, picric acid 15%, in PIPES
467 buffer, pH 6.0), and $1 \times 10^4$ amoebae per sample were analyzed using a using a LSR II Fortessa
468 analyser. The GFP fluorescence intensity falling into a *Dictyostelium* scatter gate was quantified using
469 FlowJo software (Treestar, http://www.treestar.com).

470 Alternatively, intracellular replication of *L. pneumophila* in *D. discoideum* was quantified by
471 determining colony forming units (CFU) in the supernatant as described [71, 105]. Exponentially
472 growing amoebae were washed and resuspended in MB medium (7 g of yeast extract, 14 g of
473 thiotone E peptone, 20 mM MES in 1 l of $H_2O$, pH 6.9). Amoebae ($1 \times 10^5$ cells per well) were seeded
474 onto a 96-well plate, allowed to adhere for at least 2 h, and infected at an MOI of 0.1 with *L.*
475 *pneumophila* grown in AYE medium for 21 h and diluted in MB medium. The infection was
476 synchronized by centrifugation, and the infected amoebae were incubated at 25°C. At the time
477 points indicated, the number of bacteria released into the supernatant was quantified by plating
478 aliquots (10–20 µl) of appropriate dilutions on CYE plates. Intracellular bacteria were also quantified
479 by counting CFU after lysis of the infected amoebae with saponin. At the time points indicated host
480 cells were detached by vigorous pipetting and lysed by incubation with saponin (final concentration
481 – 0.8%) for 10 min. The number of bacteria released into the supernatant was quantified by plating
482 20 µl aliquots of appropriate dilutions on CYE plates.

## 483 Acknowledgments

484 The authors would like to Phill Hawkins for his endeavours to separate *Dictyostelium* $PIP_2$s

485 References


486 1. Flannagan RS, Cosio G, Grinstein S. Antimicrobial mechanisms of phagocytes and bacterial
487 evasion strategies. Nat Rev Microbiol. 2009;7(5):355-66. Epub 2009/04/17. doi:
488 10.1038/nrmicro2128. PubMed PMID: 19369951.
489 2. Di Paolo G, De Camilli P. Phosphoinositides in cell regulation and membrane dynamics.
490 Nature. 2006;443(7112):651-7. doi: 10.1038/nature05185. PubMed PMID: 17035995.
491 3. Levin R, Grinstein S, Schlam D. Phosphoinositides in phagocytosis and macropinocytosis.
492 Biochim Biophys Acta. 2015;1851(6):805-23. doi: 10.1016/j.bbalip.2014.09.005. PubMed PMID:
493 25238964.
494 4. Gaullier JM, Simonsen A, D'Arrigo A, Bremnes B, Stenmark H, Aasland R. FYVE fingers bind
495 PtdIns(3)P. Nature. 1998;394(6692):432-3. doi: 10.1038/28767. PubMed PMID: 9697764.
496 5. Raiborg C, Bremnes B, Mehlum A, Gillooly DJ, D'Arrigo A, Stang E, et al. FYVE and coiled-coil
497 domains determine the specific localisation of Hrs to early endosomes. J Cell Sci. 2001;114(Pt
498 12):2255-63. PubMed PMID: 11493665.
499 6. Cabezas A, Pattni K, Stenmark H. Cloning and subcellular localization of a human
500 phosphatidylinositol 3-phosphate 5-kinase, PIKfyve/Fab1. Gene. 2006;371(1):34-41. doi:
501 10.1016/j.gene.2005.11.009. PubMed PMID: 16448788.
502 7. Michell RH, Heath VL, Lemmon MA, Dove SK. Phosphatidylinositol 3,5-bisphosphate:
503 metabolism and cellular functions. Trends Biochem Sci. 2006;31(1):52-63. doi:
504 10.1016/j.tibs.2005.11.013. PubMed PMID: 16364647.
505 8. Sbrissa D, Ikonomov OC, Shisheva A. PIKfyve, a mammalian ortholog of yeast Fab1p lipid
506 kinase, synthesizes 5-phosphoinositides. Effect of insulin. J Biol Chem. 1999;274(31):21589-97.
507 PubMed PMID: 10419465.
508 9. Zolov SN, Bridges D, Zhang Y, Lee WW, Riehle E, Verma R, et al. In vivo, Pikfyve generates
509 PI(3,5)P2, which serves as both a signaling lipid and the major precursor for PI5P. Proc Natl Acad Sci
510 U S A. 2012;109(43):17472-7. doi: 10.1073/pnas.1203106109. PubMed PMID: 23047693; PubMed
511 Central PMCID: PMCPMC3491506.
512 10. Yamamoto A, DeWald DB, Boronenkov IV, Anderson RA, Emr SD, Koshland D. Novel PI(4)P 5-
513 kinase homologue, Fab1p, essential for normal vacuole function and morphology in yeast. Mol Biol
514 Cell. 1995;6(5):525-39. PubMed PMID: 7663021; PubMed Central PMCID: PMCPMC301213.
515 11. Takasuga S, Sasaki T. Phosphatidylinositol-3,5-bisphosphate: metabolism and physiological
516 functions. J Biochem. 2013;154(3):211-8. doi: 10.1093/jb/mvt064. PubMed PMID: 23857703.
517 12. McCartney AJ, Zhang Y, Weisman LS. Phosphatidylinositol 3,5-bisphosphate: low abundance,
518 high significance. BioEssays : news and reviews in molecular, cellular and developmental biology.
519 2014;36(1):52-64. doi: 10.1002/bies.201300012. PubMed PMID: 24323921; PubMed Central PMCID:
520 PMCPMC3906640.
521 13. Ho CY, Alghamdi TA, Botelho RJ. Phosphatidylinositol-3,5-bisphosphate: no longer the poor
522 PIP2. Traffic. 2012;13(1):1-8. doi: 10.1111/j.1600-0854.2011.01246.x. PubMed PMID: 21736686.
523 14. Michell RH. Inositol lipids: from an archaeal origin to phosphatidylinositol 3,5-bisphosphate
524 faults in human disease. FEBS J. 2013;280(24):6281-94. doi: 10.1111/febs.12452. PubMed PMID:
525 23902363.
526 15. Ikonomov O, Sbrissa D, Shisheva A. Mammalian cell morphology and endocytic membrane
527 homeostasis require enzymatically active phosphoinositide 5-kinase PIKfyve. J Biol Chem.
528 2001;276(28):26141-7. doi: 10.1074/jbc.M101722200. PubMed PMID: 11285266.
529 16. Ikonomov OC, Sbrissa D, Mlak K, Deeb R, Fligger J, Soans A, et al. Active PIKfyve associates
530 with and promotes the membrane attachment of the late endosome-to-trans-Golgi network
531 transport factor Rab9 effector p40. J Biol Chem. 2003;278(51):50863-71. doi:
532 10.1074/jbc.M307260200. PubMed PMID: 14530284.
533 17. Rutherford AC, Traer C, Wassmer T, Pattni K, Bujny MV, Carlton JG, et al. The mammalian
534 phosphatidylinositol 3-phosphate 5-kinase (PIKfyve) regulates endosome-to-TGN retrograde

535 transport. J Cell Sci. 2006;119(Pt 19):3944-57. doi: 10.1242/jcs.03153. PubMed PMID: 16954148;
536 PubMed Central PMCID: PMC1904490.
537 18. de Lartigue J, Polson H, Feldman M, Shokat K, Tooze SA, UrbÃ© S, et al. PIKfyve Regulation
538 of Endosome-Linked Pathways. Traffic. 2009;10(7):883-93. doi: 10.1111/j.1600-0854.2009.00915.x.
539 19. Martin S, Harper CB, May LM, Coulson EJ, Meunier FA, Osborne SL. Inhibition of PIKfyve by
540 YM-201636 dysregulates autophagy and leads to apoptosis-independent neuronal cell death. PLoS
541 One. 2013;8(3):e60152. doi: 10.1371/journal.pone.0060152. PubMed PMID: 23544129; PubMed
542 Central PMCID: PMC3609765.
543 20. Rusten T, Vaccari T, Lindmo K, Rodahl L, Nezis I, Sem-Jacobsen C, et al. ESCRTs and Fab1
544 regulate distinct steps of autophagy. Curr Biol. 2007;17(20):1817-25. doi:
545 10.1016/j.cub.2007.09.032. PubMed PMID: 17935992.
546 21. Tsuruta F, Green EM, Rousset M, Dolmetsch RE. PIKfyve regulates CaV1.2 degradation and
547 prevents excitotoxic cell death. J Cell Biol. 2009;187(2):279-94. doi: 10.1083/jcb.200903028.
548 PubMed PMID: 19841139; PubMed Central PMCID: PMC2768838.
549 22. Min SH, Suzuki A, Stalker TJ, Zhao L, Wang Y, McKennan C, et al. Loss of PIKfyve in platelets
550 causes a lysosomal disease leading to inflammation and thrombosis in mice. Nat Commun.
551 2014;5:4691. doi: 10.1038/ncomms5691. PubMed PMID: 25178411; PubMed Central PMCID:
552 PMCPMC4369914.
553 23. Zhang X, Chow CY, Sahenk Z, Shy ME, Meisler MH, Li J. Mutation of FIG4 causes a rapidly
554 progressive, asymmetric neuronal degeneration. Brain : a journal of neurology. 2008;131(Pt 8):1990-
555 2001. doi: 10.1093/brain/awn114. PubMed PMID: 18556664; PubMed Central PMCID: PMC2724900.
556 24. Zhang Y, McCartney AJ, Zolov SN, Ferguson CJ, Meisler MH, Sutton MA, et al. Modulation of
557 synaptic function by VAC14, a protein that regulates the phosphoinositides PI(3,5)P(2) and PI(5)P.
558 EMBO J. 2012;31(16):3442-56. doi: 10.1038/emboj.2012.200. PubMed PMID: 22842785; PubMed
559 Central PMCID: PMC3419932.
560 25. Zhang Y, Zolov SN, Chow CY, Slutsky SG, Richardson SC, Piper RC, et al. Loss of Vac14, a
561 regulator of the signaling lipid phosphatidylinositol 3,5-bisphosphate, results in neurodegeneration
562 in mice. Proc Natl Acad Sci U S A. 2007;104(44):17518-23. doi: 10.1073/pnas.0702275104. PubMed
563 PMID: 17956977; PubMed Central PMCID: PMC2077288.
564 26. Bohdanowicz M, Grinstein S. Role of phospholipids in endocytosis, phagocytosis, and
565 macropinocytosis. Physiological reviews. 2013;93(1):69-106. doi: 10.1152/physrev.00002.2012.
566 PubMed PMID: 23303906.
567 27. Ellson CD, Anderson KE, Morgan G, Chilvers ER, Lipp P, Stephens LR, et al.
568 Phosphatidylinositol 3-phosphate is generated in phagosomal membranes. Curr Biol.
569 2001;11(20):1631-5. PubMed PMID: 11676926.
570 28. Vieira OV, Botelho RJ, Rameh L, Brachmann SM, Matsuo T, Davidson HW, et al. Distinct roles
571 of class I and class III phosphatidylinositol 3-kinases in phagosome formation and maturation. J Cell
572 Biol. 2001;155(1):19-25. doi: 10.1083/jcb.200107069. PubMed PMID: 11581283; PubMed Central
573 PMCID: PMCPMC2150784.
574 29. Fratti RA, Backer JM, Gruenberg J, Corvera S, Deretic V. Role of phosphatidylinositol 3-kinase
575 and Rab5 effectors in phagosomal biogenesis and mycobacterial phagosome maturation arrest. J Cell
576 Biol. 2001;154(3):631-44. doi: 10.1083/jcb.200106049. PubMed PMID: 11489920; PubMed Central
577 PMCID: PMCPMC2196432.
578 30. Cai X, Xu Y, Cheung AK, Tomlinson RC, Alcazar-Roman A, Murphy L, et al. PIKfyve, a class III PI
579 kinase, is the target of the small molecular IL-12/IL-23 inhibitor apilimod and a player in Toll-like
580 receptor signaling. Chem Biol. 2013;20(7):912-21. doi: 10.1016/j.chembiol.2013.05.010. PubMed
581 PMID: 23890009.
582 31. Ikonomov OC, Sbrissa D, Shisheva A. YM201636, an inhibitor of retroviral budding and
583 PIKfyve-catalyzed PtdIns(3,5)P2 synthesis, halts glucose entry by insulin in adipocytes. Biochem
584 Biophys Res Commun. 2009;382(3):566-70. doi: 10.1016/j.bbrc.2009.03.063. PubMed PMID:
585 19289105; PubMed Central PMCID: PMC3910513.

586 32. Hazeki K, Nigorikawa K, Takaba Y, Segawa T, Nukuda A, Masuda A, et al. Essential roles of
587 PIKfyve and PTEN on phagosomal phosphatidylinositol 3-phosphate dynamics. FEBS Lett.
588 2012;586(22):4010-5. doi: 10.1016/j.febslet.2012.09.043. PubMed PMID: 23068606.
589 33. Kim GH, Dayam RM, Prashar A, Terebiznik M, Botelho RJ. PIKfyve Inhibition Interferes with
590 Phagosome and Endosome Maturation in Macrophages. Traffic. 2014;15(10):1143-63. doi:
591 10.1111/tra.12199. PubMed PMID: 25041080.
592 34. Choy CH, Saffi G, Gray MA, Wallace C, Dayam RM, Ou ZA, et al. Lysosome enlargement
593 during inhibition of the lipid kinase PIKfyve proceeds through lysosome coalescence. J Cell Sci.
594 2018;131(10). Epub 2018/04/18. doi: 10.1242/jcs.213587. PubMed PMID: 29661845.
595 35. Dayam RM, Sun CX, Choy CH, Mancuso G, Glogauer M, Botelho RJ. The Lipid Kinase PIKfyve
596 Coordinates the Neutrophil Immune Response through the Activation of the Rac GTPase. Journal of
597 immunology. 2017;199(6):2096-105. Epub 2017/08/06. doi: 10.4049/jimmunol.1601466. PubMed
598 PMID: 28779020.
599 36. Nicot AS, Fares H, Payrastre B, Chisholm AD, Labouesse M, Laporte J. The phosphoinositide
600 kinase PIKfyve/Fab1p regulates terminal lysosome maturation in Caenorhabditis elegans. Mol Biol
601 Cell. 2006;17(7):3062-74. doi: 10.1091/mbc.E06-12-1120. PubMed PMID: 16801682; PubMed
602 Central PMCID: PMCPMC1483040.
603 37. Jefferies HB, Cooke FT, Jat P, Boucheron C, Koizumi T, Hayakawa M, et al. A selective PIKfyve
604 inhibitor blocks PtdIns(3,5)P(2) production and disrupts endomembrane transport and retroviral
605 budding. EMBO reports. 2008;9(2):164-70. doi: 10.1038/sj.embor.7401155. PubMed PMID:
606 18188180; PubMed Central PMCID: PMCPMC2246419.
607 38. Krishna S, Palm W, Lee Y, Yang W, Bandyopadhyay U, Xu H, et al. PIKfyve Regulates Vacuole
608 Maturation and Nutrient Recovery following Engulfment. Dev Cell. 2016;38(5):536-47. doi:
609 10.1016/j.devcel.2016.08.001. PubMed PMID: 27623384; PubMed Central PMCID:
610 PMCPMC5046836.
611 39. Ho CY, Choy CH, Wattson CA, Johnson DE, Botelho RJ. The Fab1/PIKfyve Phosphoinositide
612 Phosphate Kinase Is Not Necessary to Maintain the pH of Lysosomes and of the Yeast Vacuole. J Biol
613 Chem. 2015;290(15):9919-28. doi: 10.1074/jbc.M114.613984. PubMed PMID: 25713145.
614 40. Clark J, Kay RR, Kielkowska A, Niewczas I, Fets L, Oxley D, et al. Dictyostelium uses ether-
615 linked inositol phospholipids for intracellular signalling. EMBO J. 2014;33(19):2188-200. doi:
616 10.15252/embj.201488677. PubMed PMID: 25180230; PubMed Central PMCID: PMCPMC4282506.
617 41. Calvo-Garrido J, King JS, Munoz-Braceras S, Escalante R. Vmp1 regulates PtdIns3P signaling
618 during autophagosome formation in Dictyostelium discoideum. Traffic. 2014;15(11):1235-46. doi:
619 10.1111/tra.12210. PubMed PMID: 25131297.
620 42. King JS, Teo R, Ryves J, Reddy JV, Peters O, Orabi B, et al. The mood stabiliser lithium
621 suppresses PIP3 signalling in Dictyostelium and human cells. Dis Model Mech. 2009;2(5-6):306-12.
622 doi: 10.1242/dmm.001271. PubMed PMID: 19383941; PubMed Central PMCID: PMC2675811.
623 43. Kortholt A, King JS, Keizer-Gunnink I, Harwood AJ, Van Haastert PJ. Phospholipase C
624 regulation of phosphatidylinositol 3,4,5-trisphosphate-mediated chemotaxis. Mol Biol Cell.
625 2007;18(12):4772-9. doi: 10.1091/mbc.E07-05-0407. PubMed PMID: 17898079; PubMed Central
626 PMCID: PMC2096598.
627 44. Dormann D, Weijer G, Dowler S, Weijer CJ. In vivo analysis of 3-phosphoinositide dynamics
628 during Dictyostelium phagocytosis and chemotaxis. J Cell Sci. 2004;117(Pt 26):6497-509. doi:
629 10.1242/jcs.01579. PubMed PMID: 15572406.
630 45. Nicot AS, Fares H, Payrastre B, Chisholm AD, Labouesse M, Laporte J. The phosphoinositide
631 kinase PIKfyve/Fab1p regulates terminal lysosome maturation in Caenorhabditis elegans. Molecular
632 biology of the cell. 2006;17(7):3062-74. PubMed PMID: WOS:000238721000018.
633 46. Smith EW, Lima WC, Charette SJ, Cosson P. Effect of starvation on the endocytic pathway in
634 Dictyostelium cells. Eukaryot Cell. 2010;9(3):387-92. doi: 10.1128/EC.00285-09. PubMed PMID:
635 20097741; PubMed Central PMCID: PMCPMC2837978.

636 47. Veltman DM, Williams TD, Bloomfield G, Chen BC, Betzig E, Insall RH, et al. A plasma
637 membrane template for macropinocytic cups. eLife. 2016;5. doi: 10.7554/eLife.20085. PubMed
638 PMID: 27960076; PubMed Central PMCID: PMCPMC5154761.
639 48. Clarke M, Kohler J, Arana Q, Liu T, Heuser J, Gerisch G. Dynamics of the vacuolar H(+)-ATPase
640 in the contractile vacuole complex and the endosomal pathway of Dictyostelium cells. J Cell Sci.
641 2002;115(Pt 14):2893-905. PubMed PMID: 12082150.
642 49. Buckley CM, Gopaldass N, Bosmani C, Johnston SA, Soldati T, Insall RH, et al. WASH drives
643 early recycling from macropinosomes and phagosomes to maintain surface phagocytic receptors.
644 Proc Natl Acad Sci U S A. 2016;113(40):E5906-E15. doi: 10.1073/pnas.1524532113. PubMed PMID:
645 27647881.
646 50. Gary JD, Wurmser AE, Bonangelino CJ, Weisman LS, Emr SD. Fab1p is essential for PtdIns(3)P
647 5-kinase activity and the maintenance of vacuolar size and membrane homeostasis. J Cell Biol.
648 1998;143(1):65-79. PubMed PMID: 9763421; PubMed Central PMCID: PMC2132800.
649 51. Kerr MC, Wang JT, Castro NA, Hamilton NA, Town L, Brown DL, et al. Inhibition of the PtdIns
650 (5) kinase PIKfyve disrupts intracellular replication of Salmonella. The EMBO journal.
651 2010;29(8):1331-47.
652 52. Bak G, Lee EJ, Lee Y, Kato M, Segami S, Sze H, et al. Rapid structural changes and acidification
653 of guard cell vacuoles during stomatal closure require phosphatidylinositol 3,5-bisphosphate. Plant
654 Cell. 2013;25(6):2202-16. doi: 10.1105/tpc.113.110411. PubMed PMID: 23757398; PubMed Central
655 PMCID: PMC3723621.
656 53. Sattler N, Monroy R, Soldati T. Quantitative analysis of phagocytosis and phagosome
657 maturation. Methods in molecular biology. 2013;983:383-402. doi: 10.1007/978-1-62703-302-2_21.
658 PubMed PMID: 23494319.
659 54. Li SC, Diakov TT, Xu T, Tarsio M, Zhu W, Couoh-Cardel S, et al. The signaling lipid PI(3,5)P(2)
660 stabilizes V(1)-V(o) sector interactions and activates the V-ATPase. Mol Biol Cell. 2014;25(8):1251-62.
661 doi: 10.1091/mbc.E13-10-0563. PubMed PMID: 24523285; PubMed Central PMCID:
662 PMCPMC3982991.
663 55. Park L, Thomason PA, Zech T, King JS, Veltman DM, Carnell M, et al. Cyclical action of the
664 WASH complex: FAM21 and capping protein drive WASH recycling, not initial recruitment. Dev Cell.
665 2013;24(2):169-81. doi: 10.1016/j.devcel.2012.12.014. PubMed PMID: 23369714.
666 56. Gopaldass N, Patel D, Kratzke R, Dieckmann R, Hausherr S, Hagedorn M, et al. Dynamin A,
667 Myosin IB and Abp1 couple phagosome maturation to F-actin binding. Traffic. 2012;13(1):120-30.
668 doi: 10.1111/j.1600-0854.2011.01296.x. PubMed PMID: 22008230.
669 57. Clarke M, Maddera L, Engel U, Gerisch G. Retrieval of the vacuolar H-ATPase from
670 phagosomes revealed by live cell imaging. PLoS One. 2010;5(1):e8585. doi:
671 10.1371/journal.pone.0008585. PubMed PMID: 20052281; PubMed Central PMCID:
672 PMCPMC2796722.
673 58. Simonsen A, Lippe R, Christoforidis S, Gaullier JM, Brech A, Callaghan J, et al. EEA1 links
674 PI(3)K function to Rab5 regulation of endosome fusion. Nature. 1998;394(6692):494-8. doi:
675 10.1038/28879. PubMed PMID: 9697774.
676 59. Gillooly DJ, Morrow IC, Lindsay M, Gould R, Bryant NJ, Gaullier JM, et al. Localization of
677 phosphatidylinositol 3-phosphate in yeast and mammalian cells. Embo Journal. 2000;19(17):4577-
678 88. doi: 10.1093/emboj/19.17.4577. PubMed PMID: WOS:000089275600016.
679 60. Leiba J, Sabra A, Bodinier R, Marchetti A, Lima WC, Melotti A, et al. Vps13F links bacterial
680 recognition and intracellular killing in Dictyostelium. Cell Microbiol. 2017. doi: 10.1111/cmi.12722.
681 PubMed PMID: 28076662.
682 61. Froquet R, Lelong E, Marchetti A, Cosson P. Dictyostelium discoideum: a model host to
683 measure bacterial virulence. Nat Protoc. 2009;4(1):25-30. doi: 10.1038/nprot.2008.212. PubMed
684 PMID: 19131953.

685 62. Hilbi H, Hoffmann C, Harrison CF. Legionella spp. outdoors: colonization, communication and
686 persistence. Environ Microbiol Rep. 2011;3(3):286-96. doi: 10.1111/j.1758-2229.2011.00247.x.
687 PubMed PMID: 23761274.
688 63. Finsel I, Hilbi H. Formation of a pathogen vacuole according to Legionella pneumophila: how
689 to kill one bird with many stones. Cell Microbiol. 2015;17(7):935-50. doi: 10.1111/cmi.12450.
690 PubMed PMID: 25903720.
691 64. Ge J, Shao F. Manipulation of host vesicular trafficking and innate immune defence by
692 Legionella Dot/Icm effectors. Cell Microbiol. 2011;13(12):1870-80. doi: 10.1111/j.1462-
693 5822.2011.01710.x. PubMed PMID: 21981078.
694 65. Weber S, Wagner M, Hilbi H. Live-cell imaging of phosphoinositide dynamics and membrane
695 architecture during Legionella infection. MBio. 2014;5(1):e00839-13. doi: 10.1128/mBio.00839-13.
696 PubMed PMID: 24473127; PubMed Central PMCID: PMCPMC3903275.
697 66. Brombacher E, Urwyler S, Ragaz C, Weber SS, Kami K, Overduin M, et al. Rab1 guanine
698 nucleotide exchange factor SidM is a major phosphatidylinositol 4-phosphate-binding effector
699 protein of Legionella pneumophila. J Biol Chem. 2009;284(8):4846-56. doi:
700 10.1074/jbc.M807505200. PubMed PMID: 19095644; PubMed Central PMCID: PMC2643517.
701 67. Hilbi H, Weber S, Finsel I. Anchors for effectors: subversion of phosphoinositide lipids by
702 legionella. Front Microbiol. 2011;2:91. doi: 10.3389/fmicb.2011.00091. PubMed PMID: 21833330;
703 PubMed Central PMCID: PMC3153050.
704 68. Jank T, Bohmer KE, Tzivelekidis T, Schwan C, Belyi Y, Aktories K. Domain organization of
705 Legionella effector SetA. Cell Microbiol. 2012;14(6):852-68. doi: 10.1111/j.1462-5822.2012.01761.x.
706 PubMed PMID: 22288428.
707 69. Finsel I, Ragaz C, Hoffmann C, Harrison CF, Weber S, van Rahden VA, et al. The Legionella
708 effector RidL inhibits retrograde trafficking to promote intracellular replication. Cell Host Microbe.
709 2013;14(1):38-50. doi: 10.1016/j.chom.2013.06.001. PubMed PMID: 23870312.
710 70. Harding CR, Mattheis C, Mousnier A, Oates CV, Hartland EL, Frankel G, et al. LtpD Is a Novel
711 Legionella pneumophila Effector That Binds Phosphatidylinositol 3-Phosphate and Inositol
712 Monophosphatase IMPA1. Infection and Immunity. 2013;81(11):4261-70. doi: 10.1128/iai.01054-13.
713 PubMed PMID: WOS:000325719900031.
714 71. Weber SS, Ragaz C, Reus K, Nyfeler Y, Hilbi H. Legionella pneumophila exploits PI(4)P to
715 anchor secreted effector proteins to the replicative vacuole. Plos Pathogens. 2006;2(5):418-30. doi:
716 ARTN e46

717 10.1371/journal.ppat.0020046. PubMed PMID: WOS:000202894500009.
718 72. Dolinsky S, Haneburger I, Cichy A, Hannemann M, Itzen A, Hilbi H. The Legionella
719 longbeachae Icm/Dot substrate SidC selectively binds phosphatidylinositol 4-phosphate with
720 nanomolar affinity and promotes pathogen vacuole-endoplasmic reticulum interactions. Infect
721 Immun. 2014;82(10):4021-33. doi: 10.1128/IAI.01685-14. PubMed PMID: 25024371; PubMed
722 Central PMCID: PMCPMC4187854.
723 73. Segal G, Shuman HA. Intracellular multiplication and human macrophage killing by Legionella
724 pneumophila are inhibited by conjugal components of IncQ plasmid RSF1010. Molecular
725 Microbiology. 1998;30(1):197-208. doi: 10.1046/j.1365-2958.1998.01054.x. PubMed PMID:
726 WOS:000076538500017.
727 74. Hilbi H, Segal G, Shuman HA. Icm/dot-dependent upregulation of phagocytosis by Legionella
728 pneumophila. Mol Microbiol. 2001;42(3):603-17. PubMed PMID: 11722729.
729 75. Rizopoulos Z, Balistreri G, Kilcher S, Martin CK, Syedbasha M, Helenius A, et al. Vaccinia Virus
730 Infection Requires Maturation of Macropinosomes. Traffic. 2015;16(8):814-31. doi:
731 10.1111/tra.12290. PubMed PMID: 25869659; PubMed Central PMCID: PMCPMC4973667.
732 76. Sbrissa D, Ikonomov OC, Shisheva A. PIKfyve lipid kinase is a protein kinase: downregulation
733 of 5'-phosphoinositide product formation by autophosphorylation. Biochemistry.
734 2000;39(51):15980-9. Epub 2000/12/22. PubMed PMID: 11123925.

735 77. Dong XP, Shen D, Wang X, Dawson T, Li X, Zhang Q, et al. PI(3,5)P(2) controls membrane
736 trafficking by direct activation of mucolipin Ca(2+) release channels in the endolysosome. Nat
737 Commun. 2010;1:38. doi: 10.1038/ncomms1037. PubMed PMID: 20802798; PubMed Central PMCID:
738 PMCPMC2928581.
739 78. Dayam RM, Saric A, Shilliday RE, Botelho RJ. The Phosphoinositide-Gated Lysosomal Ca(2+)
740 Channel, TRPML1, Is Required for Phagosome Maturation. Traffic. 2015;16(9):1010-26. doi:
741 10.1111/tra.12303. PubMed PMID: 26010303.
742 79. Li X, Rydzewski N, Hider A, Zhang X, Yang J, Wang W, et al. A molecular mechanism to
743 regulate lysosome motility for lysosome positioning and tubulation. Nat Cell Biol. 2016;18(4):404-17.
744 doi: 10.1038/ncb3324. PubMed PMID: 26950892.
745 80. Lima WC, Leuba F, Soldati T, Cosson P. Mucolipin controls lysosome exocytosis in
746 Dictyostelium. J Cell Sci. 2012;125(Pt 9):2315-22. doi: 10.1242/jcs.100362. PubMed PMID: 22357942.
747 81. Horwitz MA. THE LEGIONNAIRES-DISEASE BACTERIUM (LEGIONELLA-PNEUMOPHILA)
748 INHIBITS PHAGOSOME-LYSOSOME FUSION IN HUMAN-MONOCYTES. Journal of Experimental
749 Medicine. 1983;158(6):2108-26. doi: 10.1084/jem.158.6.2108. PubMed PMID:
750 WOS:A1983RV00200023.
751 82. Lamothe J, Huynh KK, Grinstein S, Valvano MA. Intracellular survival of Burkholderia
752 cenocepacia in macrophages is associated with a delay in the maturation of bacteria-containing
753 vacuoles. Cell Microbiol. 2007;9(1):40-53. doi: 10.1111/j.1462-5822.2006.00766.x. PubMed PMID:
754 16869828.
755 83. Smith LM, Dixon EF, May RC. The fungal pathogen Cryptococcus neoformans manipulates
756 macrophage phagosome maturation. Cell Microbiol. 2015;17(5):702-13. doi: 10.1111/cmi.12394.
757 PubMed PMID: 25394938.
758 84. Segal G, Shuman HA. Legionella pneumophila utilizes the same genes to multiply within
759 Acanthamoeba castellanii and human macrophages. Infection and Immunity. 1999;67(5):2117-24.
760 PubMed PMID: WOS:000079909300010.
761 85. Steenbergen JN, Shuman HA, Casadevall A. Cryptococcus neoformans interactions with
762 amoebae suggest an explanation for its virulence and intracellular pathogenic strategy in
763 macrophages. Proc Natl Acad Sci U S A. 2001;98(26):15245-50. doi: 10.1073/pnas.261418798.
764 PubMed PMID: 11742090; PubMed Central PMCID: PMC65014.
765 86. Hasselbring BM, Patel MK, Schell MA. Dictyostelium discoideum as a model system for
766 identification of Burkholderia pseudomallei virulence factors. Infect Immun. 2011;79(5):2079-88.
767 doi: 10.1128/IAI.01233-10. PubMed PMID: 21402765; PubMed Central PMCID: PMC3088138.
768 87. Hubber A, Roy CR. Modulation of host cell function by Legionella pneumophila type IV
769 effectors. Annu Rev Cell Dev Biol. 2010;26:261-83. doi: 10.1146/annurev-cellbio-100109-104034.
770 PubMed PMID: 20929312.
771 88. Isberg RR, O'Connor TJ, Heidtman M. The Legionella pneumophila replication vacuole:
772 making a cosy niche inside host cells. Nature Reviews Microbiology. 2009;7(1):12-24. doi:
773 10.1038/nrmicro1967. PubMed PMID: WOS:000262110300009.
774 89. Lima WC, Pillonel T, Bertelli C, Ifrid E, Greub G, Cosson P. Genome sequencing and functional
775 characterization of the non-pathogenic Klebsiella pneumoniae KpGe bacteria. Microbes and
776 infection / Institut Pasteur. 2018;20(5):293-301. Epub 2018/05/14. doi:
777 10.1016/j.micinf.2018.04.001. PubMed PMID: 29753816.
778 90. Froquet R, Lelong E, Marchetti A, Cosson P. Dictyostelium discoideum: a model host to
779 measure bacterial virulence. Nature Protocols. 2009;4(1):25-30. doi: 10.1038/nprot.2008.212.
780 PubMed PMID: WOS:000265781800003.
781 91. Wilkins A, Khosla M, Fraser DJ, Spiegelman GB, Fisher PR, Weeks G, et al. Dictyostelium RasD
782 is required for normal phototaxis, but not differentiation. Genes Dev. 2000;14(11):1407-13. PubMed
783 PMID: 10837033; PubMed Central PMCID: PMCPMC316659.
784 92. Sutoh K. A transformation vector for dictyostelium discoideum with a new selectable marker
785 bsr. Plasmid. 1993;30(2):150-4. doi: 10.1006/plas.1993.1042. PubMed PMID: 8234487.

786 93. Veltman DM, Lemieux MG, Knecht DA, Insall RH. PIP(3)-dependent macropinocytosis is
787 incompatible with chemotaxis. J Cell Biol. 2014;204(4):497-505. doi: 10.1083/jcb.201309081.
788 PubMed PMID: 24535823; PubMed Central PMCID: PMCPMC3926956.
789 94. Carnell M, Zech T, Calaminus SD, Ura S, Hagedorn M, Johnston SA, et al. Actin polymerization
790 driven by WASH causes V-ATPase retrieval and vesicle neutralization before exocytosis. J Cell Biol.
791 2011;193(5):831-9. doi: 10.1083/jcb.201009119. PubMed PMID: 21606208; PubMed Central PMCID:
792 PMC3105540.
793 95. Veltman DM, Akar G, Bosgraaf L, Van Haastert PJ. A new set of small, extrachromosomal
794 expression vectors for Dictyostelium discoideum. Plasmid. 2009;61(2):110-8. doi:
795 10.1016/j.plasmid.2008.11.003. PubMed PMID: 19063918.
796 96. King J, Insall RH. Parasexual genetics of Dictyostelium gene disruptions: identification of a ras
797 pathway using diploids. Bmc Genetics. 2003;4. doi: 10.1186/1471-2156-4-12. PubMed PMID:
798 WOS:000184659500001.
799 97. Arafah S, Kicka S, Trofimov V, Hagedorn M, Andreu N, Wiles S, et al. Setting up and
800 monitoring an infection of Dictyostelium discoideum with mycobacteria. Methods Mol Biol.
801 2013;983:403-17. doi: 10.1007/978-1-62703-302-2_22. PubMed PMID: 23494320.
802 98. Gotthardt D, Dieckmann R, Blancheteau V, Kistler C, Reichardt F, Soldati T. Preparation of
803 intact, highly purified phagosomes from Dictyostelium. Methods Mol Biol. 2006;346:439-48. doi:
804 10.1385/1-59745-144-4:439. PubMed PMID: 16957306.
805 99. Fok AK, Clarke M, Ma L, Allen RD. Vacuolar H(+)-ATPase of Dictyostelium discoideum. A
806 monoclonal antibody study. J Cell Sci. 1993;106 ( Pt 4):1103-13. Epub 1993/12/01. PubMed PMID:
807 8126094.
808 100. Journet A, Chapel A, Jehan S, Adessi C, Freeze H, Klein G, et al. Characterization of
809 Dictyostelium discoideum cathepsin D. Journal of cell science. 1999;112(21):3833-43.
810 101. Dieckmann R, von Heyden Y, Kistler C, Gopaldass N, Hausherr S, Crawley SW, et al. A myosin
811 IK-Abp1-PakB circuit acts as a switch to regulate phagocytosis efficiency. Mol Biol Cell.
812 2010;21(9):1505-18. Epub 2010/03/05. doi: 10.1091/mbc.E09-06-0485. PubMed PMID: 20200225;
813 PubMed Central PMCID: PMCPMC2861610.
814 102. Davidson AJ, King JS, Insall RH. The use of streptavidin conjugates as immunoblot loading
815 controls and mitochondrial markers for use with Dictyostelium discoideum. Biotechniques.
816 2013;55(1):39-41. doi: 10.2144/000114054. PubMed PMID: 23834384.
817 103. Sadosky AB, Wiater LA, Shuman HA. Identification of Legionella pneumophila genes required
818 for growth within and killing of human macrophages. Infect Immun. 1993;61(12):5361-73. PubMed
819 PMID: 8225610; PubMed Central PMCID: PMCPMC281323.
820 104. Feeley JC, Gibson RJ, Gorman GW, Langford NC, Rasheed JK, Mackel DC, et al. Charcoal-yeast
821 extract agar: primary isolation medium for Legionella pneumophila. J Clin Microbiol. 1979;10(4):437-
822 41. PubMed PMID: 393713; PubMed Central PMCID: PMCPMC273193.
823 105. Solomon JM, Rupper A, Cardelli JA, Isberg RR. Intracellular growth of Legionella pneumophila
824 in Dictyostelium discoideum, a system for genetic analysis of host-pathogen interactions. Infect
825 Immun. 2000;68(5):2939-47. PubMed PMID: 10768992; PubMed Central PMCID: PMCPMC97507.

826

827 ## Figure Legends

828 ### Figure 1

829 **Knockout or inhibition of PIKfyve leads to a swollen vesicle phenotype.** (A) DIC images of Ax3, two
830 independent *PIKfyve*$^-$ clones and a random integrant growing in HL5 medium. Arrows indicate the
831 enlarged vesicles. (B) Changes in morphology upon incubation in low osmolarity starvation buffer
832 (KK2) compared to full medium (HL5). Swollen vesicles in *PIKfyve*$^-$ cells became initially more
833 apparent but were lost as cells entered differentiation. (C) Induction of swollen vesicles with 5 µM
834 apilimod, a PIKfyve-specific inhibitor, images taken in HL5 medium after 5 hours of treatment.

835 ### Figure 2

836 ***PIKfyve*-null cells have growth defects**. Measurement of (A) macropinocytosis or (B) exocytosis in
837 Ax3 and *PIKfyve*$^-$ cells as measured by uptake or loss of FITC dextran. (C) Growth rates in axenic
838 culture. *PIKfyve*$^-$ cells had a significantly longer generation time than Ax3 cells (Student's t-test). (D)
839 Phagocytosis of *E. coli,* as measured by the ability of *Dictyostelium* cells to reduce the turbidity of a
840 bacterial suspension. (E) Growth *PIKfyve* mutants on lawns of *K. pneumoniae* as indicated by the
841 clearance of bacteria-free plaques on agar plates. All data plotted are mean +/- SD.

842 ### Figure 3

843 **Disruption of *PIKfyve* prevents V-ATPase delivery and phagosome acidification.** (A) Measurement
844 of phagosomal acidification in Ax2 and *PIKfyve*$^-$ cells after engulfment of beads conjugated to pH-
845 sensitive fluorophores. After initial acidification, *Dictyostelium* phagosomes reneutralise ~45 minutes
846 prior to exocytosis. (B) Recruitment of the V-ATPase subunit GFP-VatM to phagocytosed pHrodo-
847 labelled yeast visualised by confocal time-lapse imaging. (C) Quantification of GFP-VatM recruitment
848 over time averaged across multiple phagocytic events. Images were quantified by automated
849 selection of a 0.5 µm-thick ring surrounding the yeast at each time point (see yellow dotted circle in
850 (B)). N indicates the total number of cells analysed over 3 independent experiments. Quantification
851 of the associated increase in yeast-associated pHrodo fluorescence, indicating acidification is shown
852 in (D). Data shown are mean +/- SEM, p values calculated by Student's t-test.

853 ### Figure 4

854 **PIKfyve is required for hydrolase activity and proteolysis.** (A) Phagosomal proteolysis measured by
855 dequenching of DQ-BSA-conjugated beads after phagocytosis. (B) Total proteolytic activity in cell
856 lysates against DQ-BSA-beads is unchanged upon *PIKfyve* disruption, dotted lines are parallel
857 samples in the presence of protease inhibitors. (C) Western blot of cathepsin D protein levels, three
858 independent samples of each strain were normalised for total protein and are quantified in (D).

859 Loading control is fluorescent streptavidin which recognises the mitochondrial protein MCCC1; P-
860 value from a one-sample T-test. (E) Analysis of phagosome maturation, by purifying phagosomes
861 from cells after maturation for the indicated times. VatA is a subunit of the $V_1$ subcomplex of the V-
862 ATPase, whereas VatM is a $V_0$ component. Blots are from the same samples and are representative
863 of multiple independent purifications. (F) Analysis of PI(3)P dynamics in the absence of PIKfyve.
864 PI(3)P was monitored by the recruitment of GFP-2xFYVE following phagocytosis of 3 µm beads
865 (asterisks) imaged by confocal time-lapse microscopy. (G) Time that GFP-2xFYVE stays associated
866 with phagosomes following engulfment, indicating that PI(3)P removal is not PIKfyve-dependent. N
867 indicates the total number of cells quantified across 3 independent experiments. Data shown are
868 mean ± SEM (A & B) or SD (G).

869 Figure 5

870 **Bacterial survival is increased in *PIKfyve*-null cells**. (A) Stills from widefield timelapse movies of
871 *Dictyostelium* cells eating GFP-expressing *Klebsiella pneumoniae.* The point of bacterial cell
872 permeablisation and death can be inferred from the quenching of GFP fluorescence after
873 engulfment. Arrows indicate captured bacteria. This is quantified in (B) which shows a Kaplan-Meyer
874 survival graph, based on the persistence of bacteria GFP-fluorescence within the amoebae. 60
875 bacteria were followed across three independent experiments and survived significantly longer in
876 *PIKfyve*-null cells than Ax2 ($p<0.0001$, Mantel-Cox test). (C) Loss of PIKfyve inhibits growth on diverse
877 bacteria. Growth was assessed by plating serial dilutions of amoebae on lawns of different bacteria
878 and dark plaques indicate amoebae growth. Data for all bacteria are summarised in (D).

879 Figure 6

880 **PIKfyve is required to suppress *Legionella* replication.** A) Wild-type (Ax2, black lines), or *PIKfyve*-null
881 *Dictyostelium* (red lines) were infected (MOI 50) with wild-type (JR32, solid lines) or avirulent (Δ*icmT*,
882 dotted lines) *Legionella* expressing GFP and fixed 40 min post infection before analysis by flow
883 cytometry. The GFP fluorescence intensity, indicating bacteria per cell was indistinguishable
884 between the two *Dictyostelium* strains, but higher for JR32 than Δ*icmT*. Uninfected cells are
885 represented by pale black/red lines. Data are representative of three independent experiments,
886 performed in duplicate. (B) Survival of GFP-Δ*icmT Legionella* after infecting Ax2 and *PIKfyve*-null
887 amoebae (MOI 50). Bacterial colony forming units (CFU) were determined at each timepoint after
888 lysis of the *Dictyostelium* amoebae. (C) Outcome of infection with either wild-type (solid lines) or
889 Δ*icmT* (dashed lines) *Legionella*. *Dictyostelium* cells were infected at a MOI of 0.1, and intracellular
890 growth measured by CFU's at each indicated time. Data shown are the means +/- SEM of 3
891 independent experiments performed in triplicate (*=$p<0.05$, **$p<0.01$ Student's t-test vs equivalent

892 Ax2 infection). (D) Flow cytometry of intracellular bacterial burden of Ax3-derived *PIKfyve*-null cells
893 infected with GFP-producing *Legionella* strains over time. Virulent *Legionella* replicate more
894 efficiently in *PIKfyve*$^{-}$ *Dictyostelium*, as indicated by the increasing proportions of amoebae
895 containing high levels of GFP over time. Graphs show >10,000 cells measured at each time point, and
896 are representative of 3 independent experiments.

897 ## Supplementary Figure 1

898 ***PIKfyve* gene disruption.** (A) Schematic representation of *Dictyostelium* PIKfyve indicating the site
899 where the blasticidin resistance cassette was inserted into the gene to generate knockouts.

900 ## Supplementary Figure 2

901 **PIKfyve is not required for development.** (A) Images of *Dictyostelium* fruiting bodies formed on filter
902 discs, indicating a normal morphology and proportioning in the absence of PIKfyve. (B) Higher
903 magnification differential interference contrast (DIC) images of pores collected from the fruiting
904 bodies in (A).

905 ## Supplementary Figure 3

906 **Conservation of *PIKfyve*-null phenotypes in Ax2-derived mutants.** Phagocytosis of (A) of 1 µm
907 beads or (B) GFP-expressing *Mycobacterium smegmatis* measured by flow cytometry, is normal in
908 *PIKfyve*-null cells. (C) Growth on lawns of *K. pneumoniae* is impaired. Colony diameter over time is
909 plotted in (D). All data are means +/- SD.

910 ## Supplementary Figure 4

911 **VatB-GFP expression has a dominant negative effect on acidification.** (A) Western blot of cells
912 expressing VatB-GFP or GFP-VatM, probed with an anti-GFP antibody (green). There was no
913 difference in expression levels between Ax2 and *PIKfyve*$^{-}$ cells for either reporter. However, VatB-
914 GFP was expressed at higher levels than GFP-VatM, likely because it is present in 3 copies per V-
915 ATPase complex. Loading control is the mitochondrial protein MCCC1, recognised by Alexa680-
916 conjugated streptavidin (red). (B) Recruitment of vatB-GFP to phagosomes containing pHrodo-
917 labelled yeast. (C) Automated image analysis of vatB-GFP recruitment as described in Figure 3,
918 showing reduced recruitment in *PIKfyve*-null cells. (D) Phagosome acidification, measured by the
919 increase in pHrodo fluorescence over time. Note that expression of vatB-GFP in Ax2 cells significantly
920 reduces phagosome acidification relative to GFP-vatM expressing cells, indicating disruption of V-
921 ATPase activity. Values plotted are mean +/- SEM.

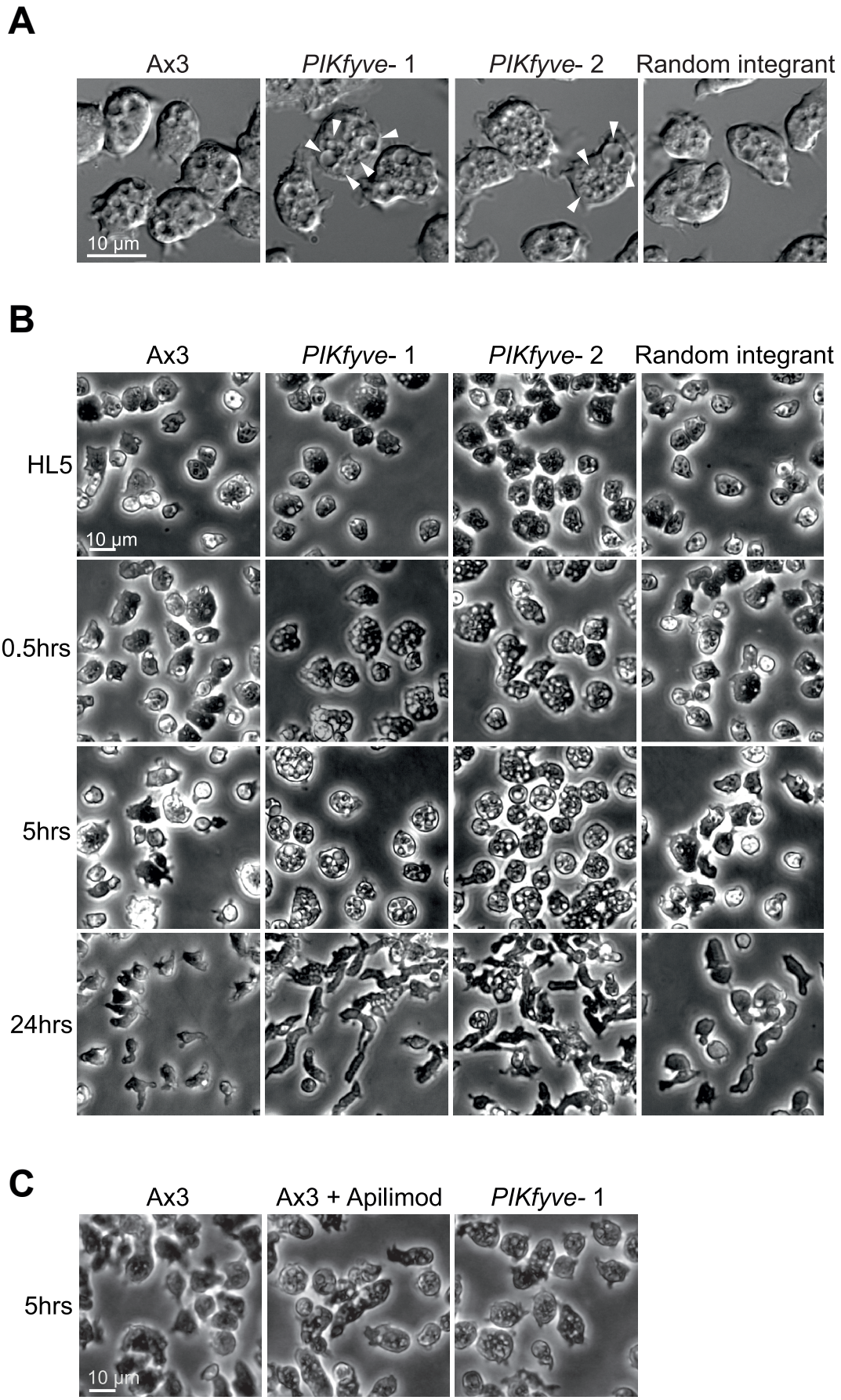


**Figure 1: KO or inhibition of PIKfyve leads to a swollen vesicle phenotype**

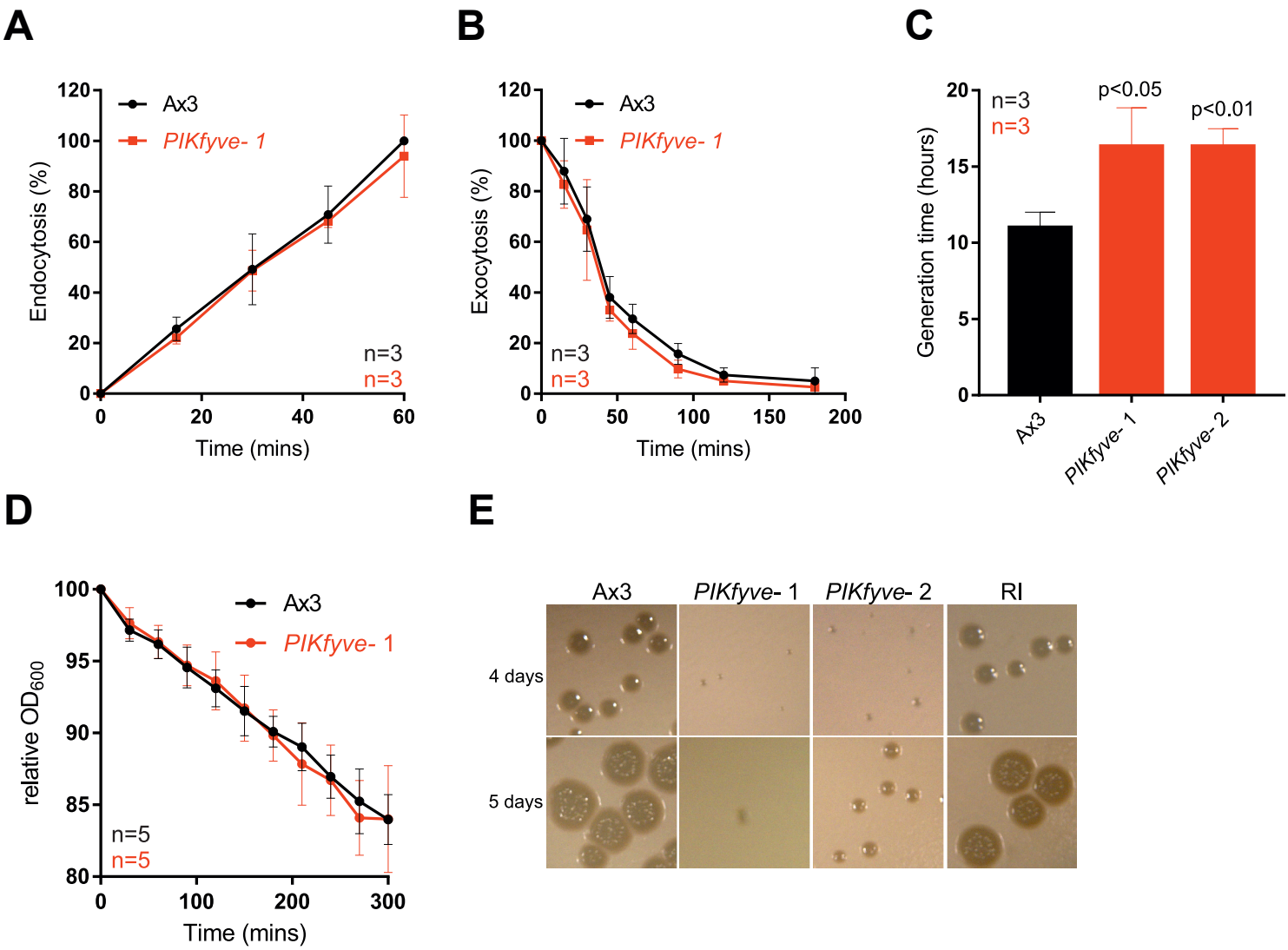


**Figure 2: *PIKfyve*- cells have growth defects**

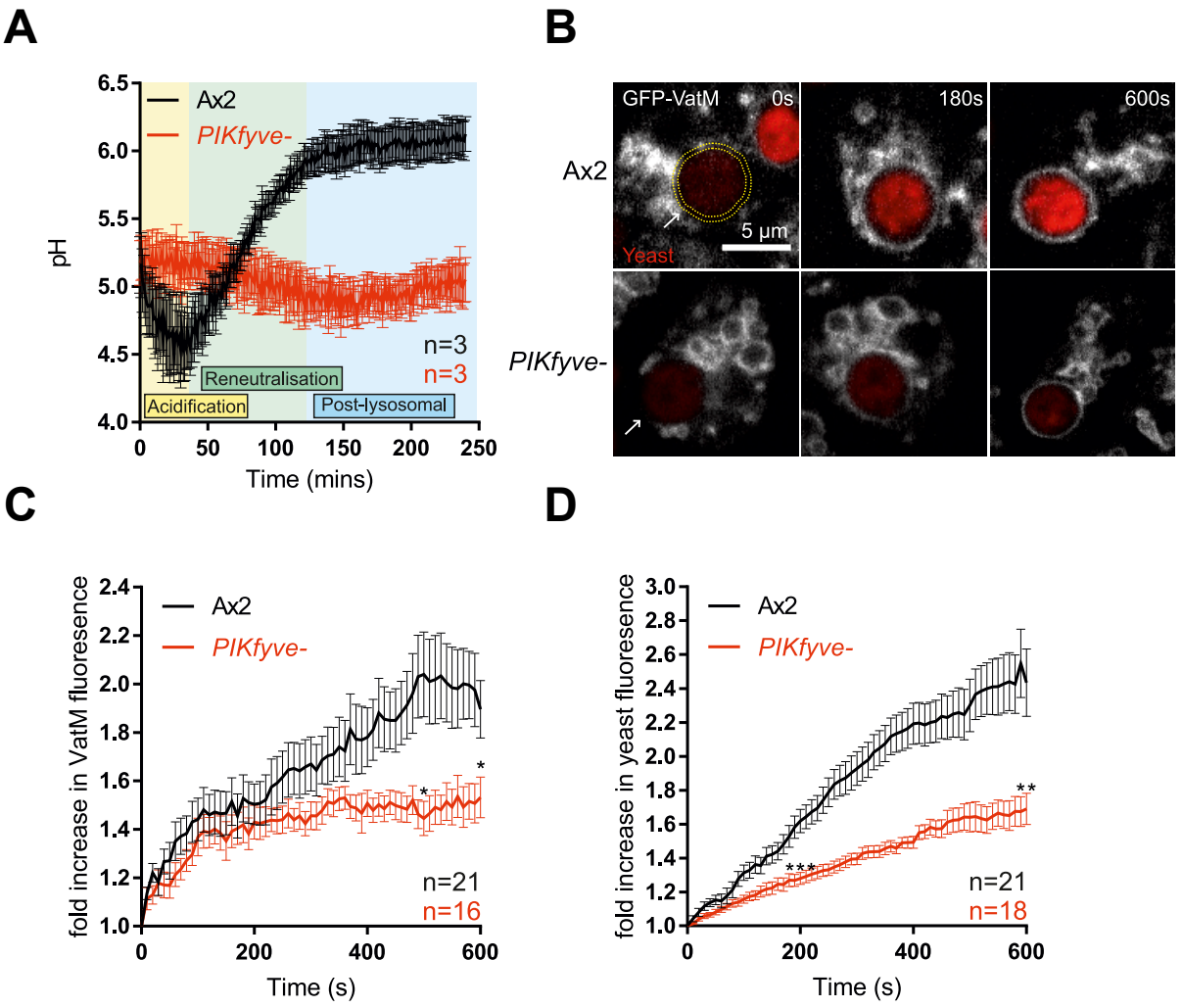


**Figure 3: Disruption of PIKfyve prevents v-ATPase delivery and phagosome acidification**

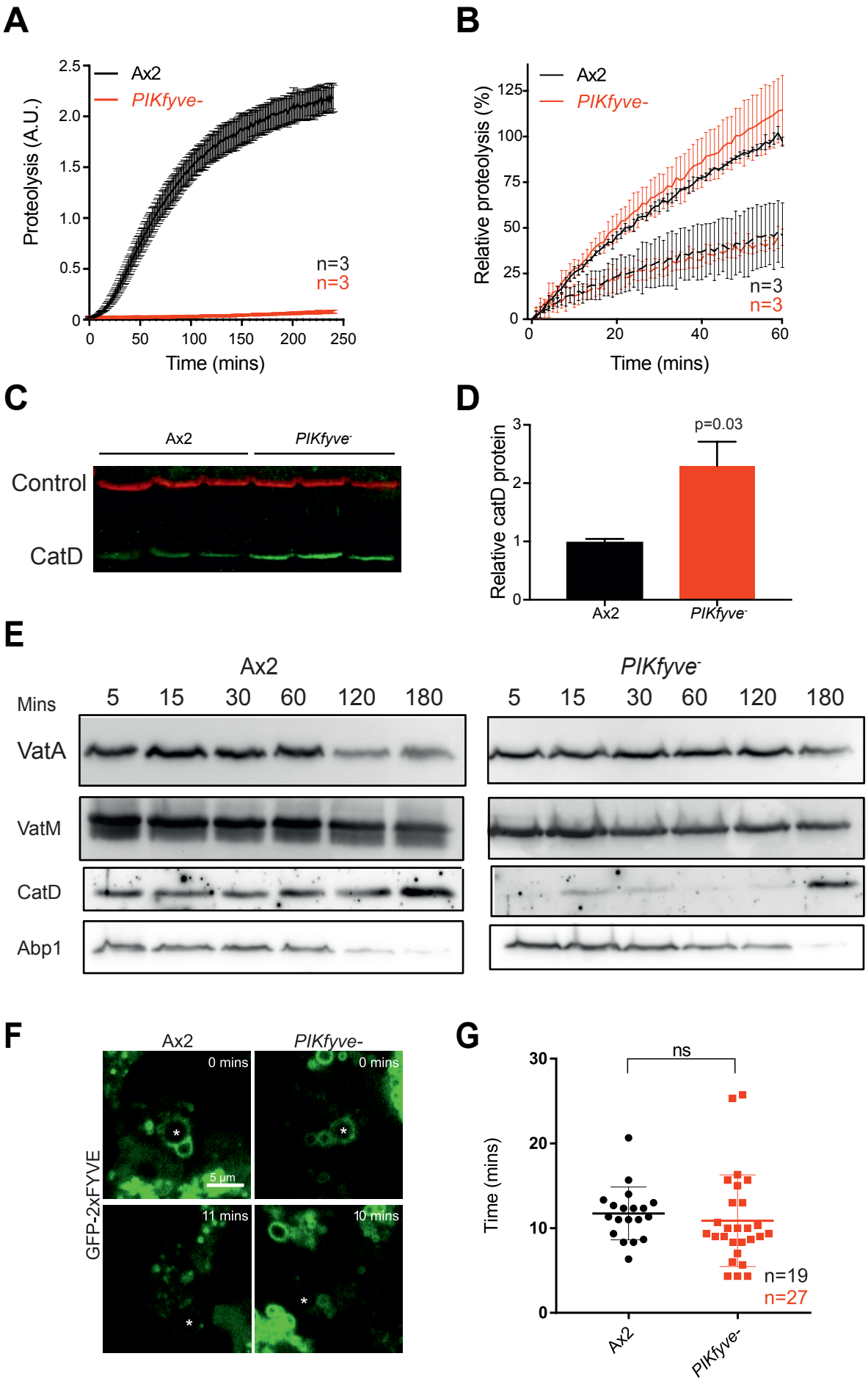


**Figure 4: PIKfyve is required for proteolysis and hydrolase delivery**

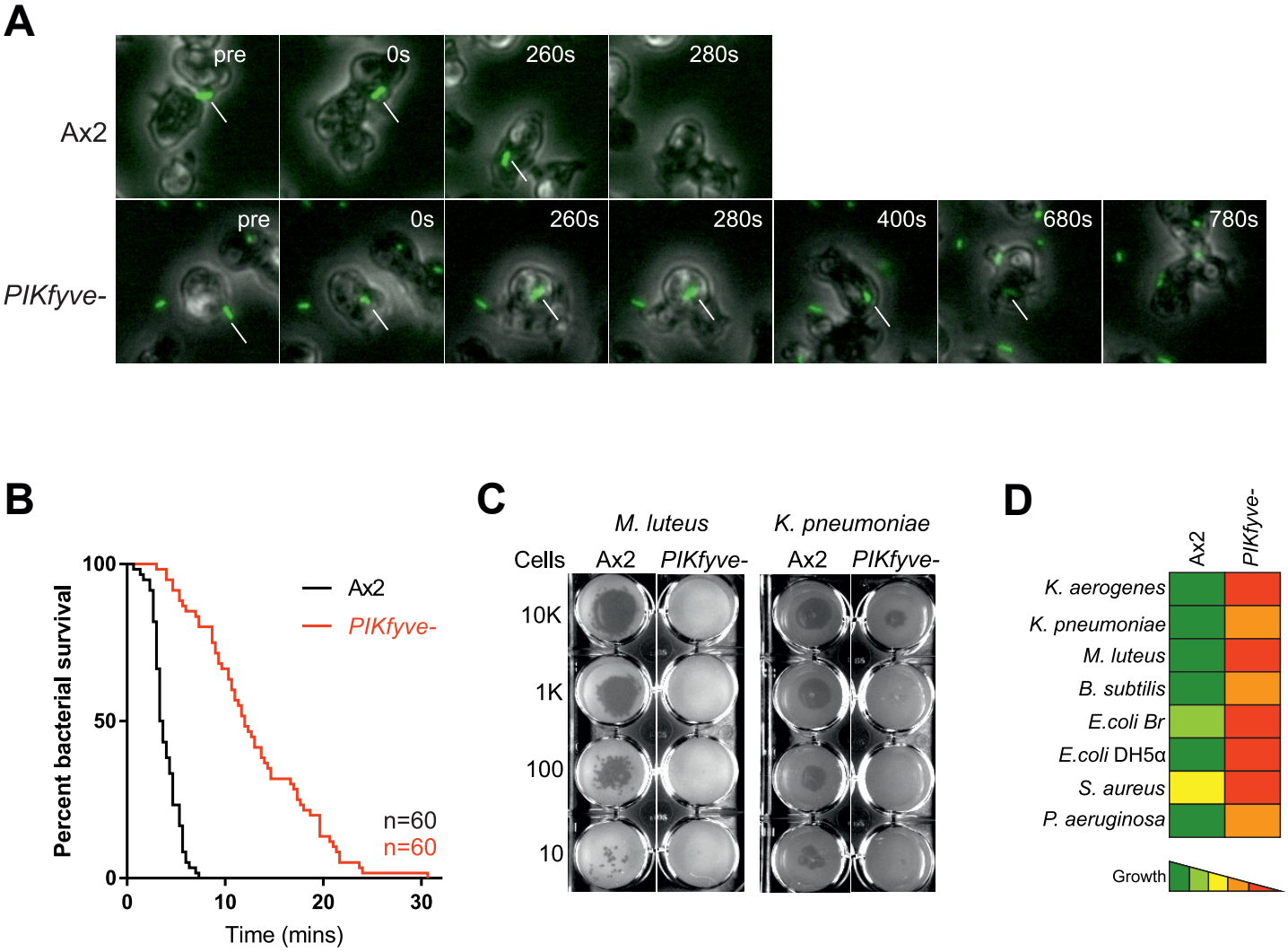


**Figure 5: Bacterial survival is increased in *PIKfyve*⁻ cells**

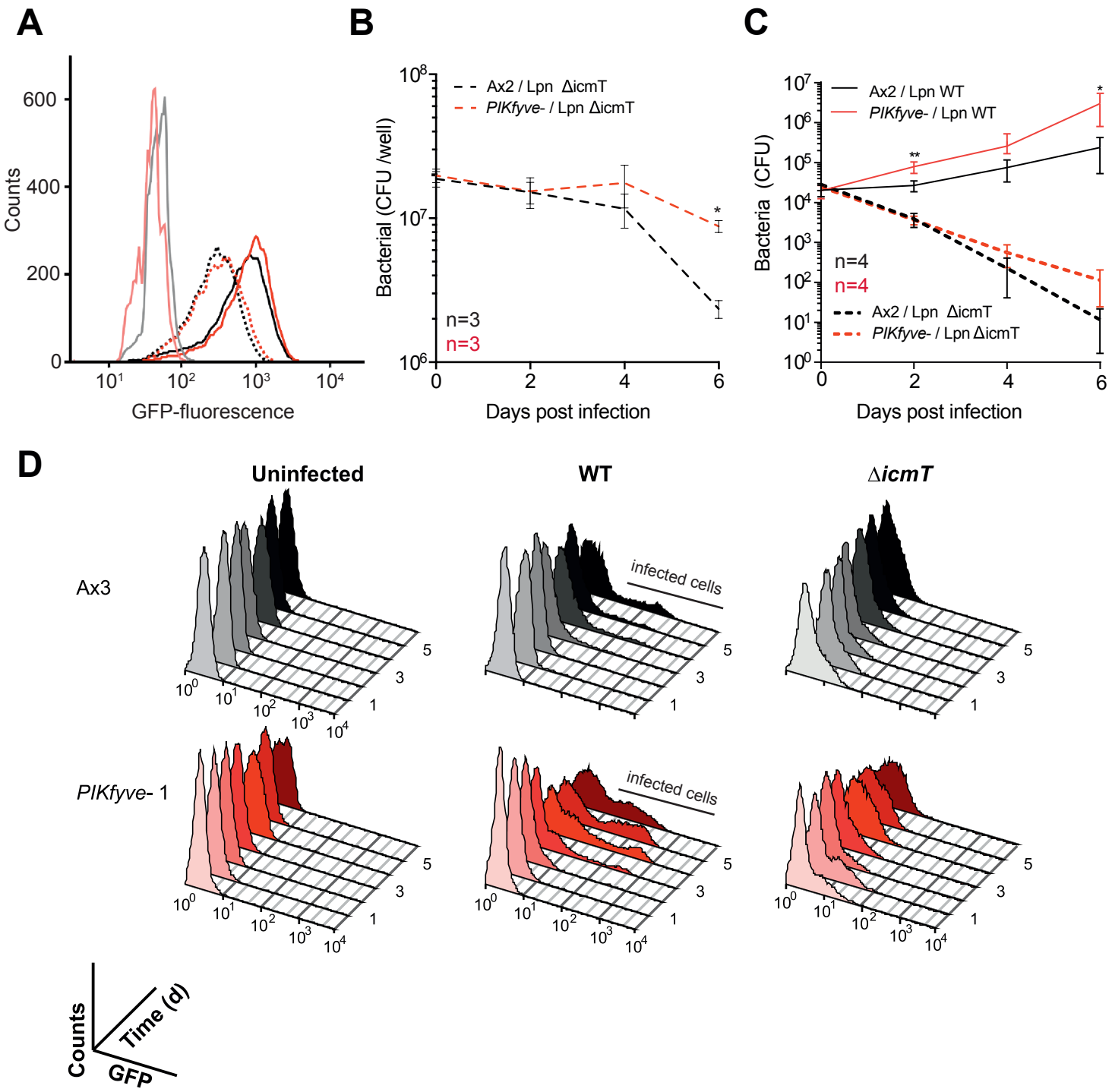


**Figure 6: *PIKfyve* is required to suppress *Legionella* infection**

A

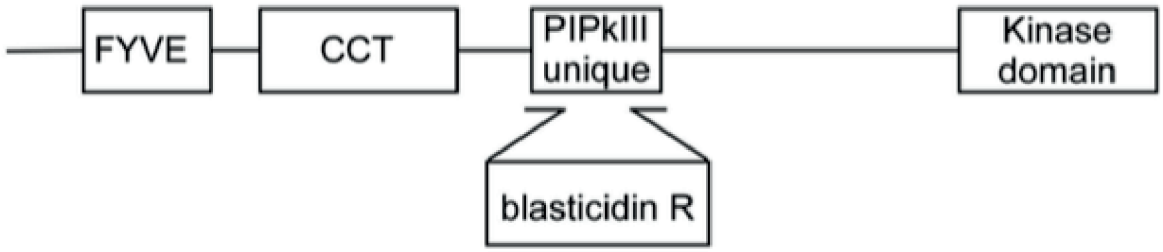


# Supplementary figure 1: PIKfyve gene disruption

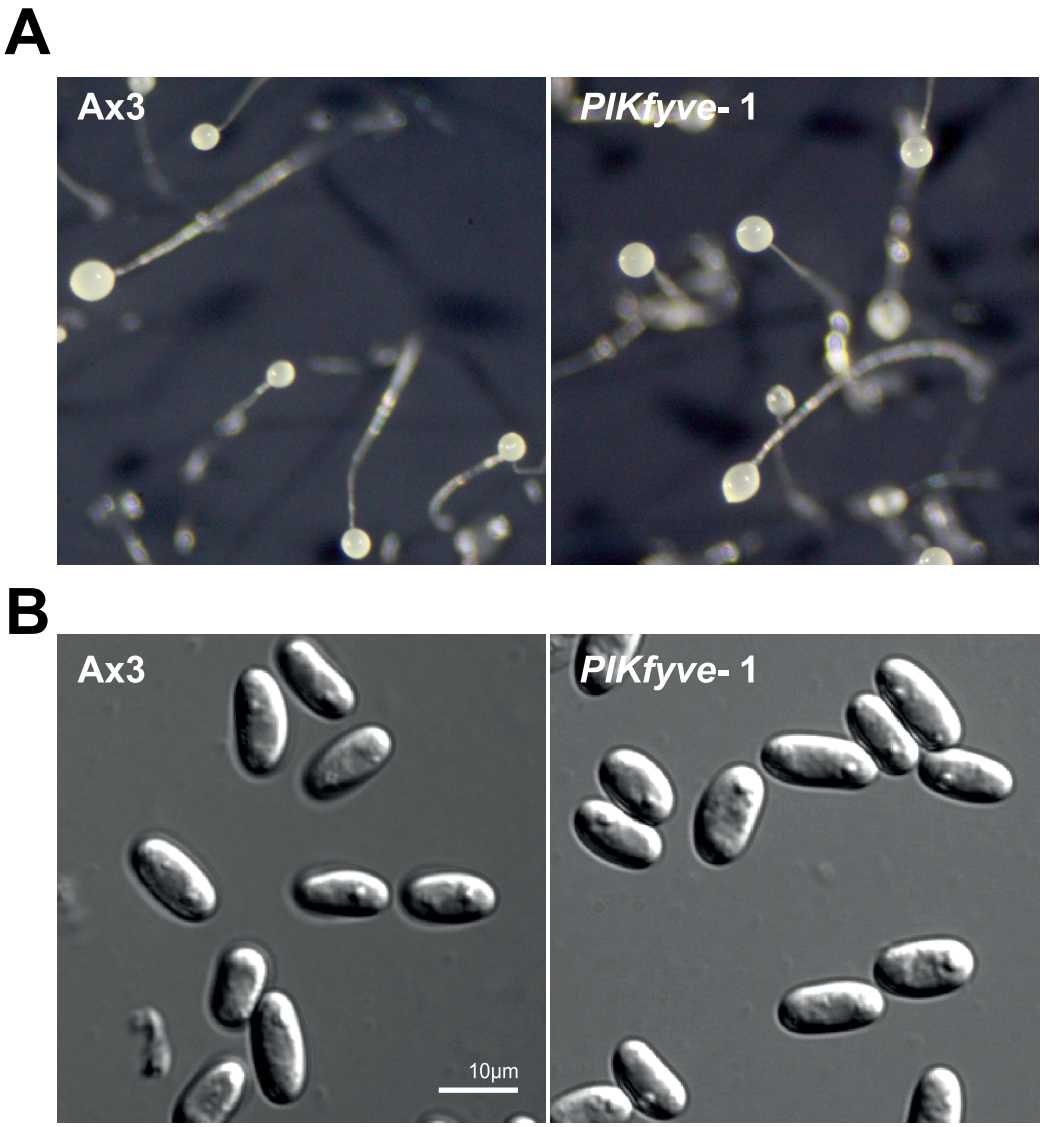


**Supplementary figure 2: PIKfyve is not required for development**

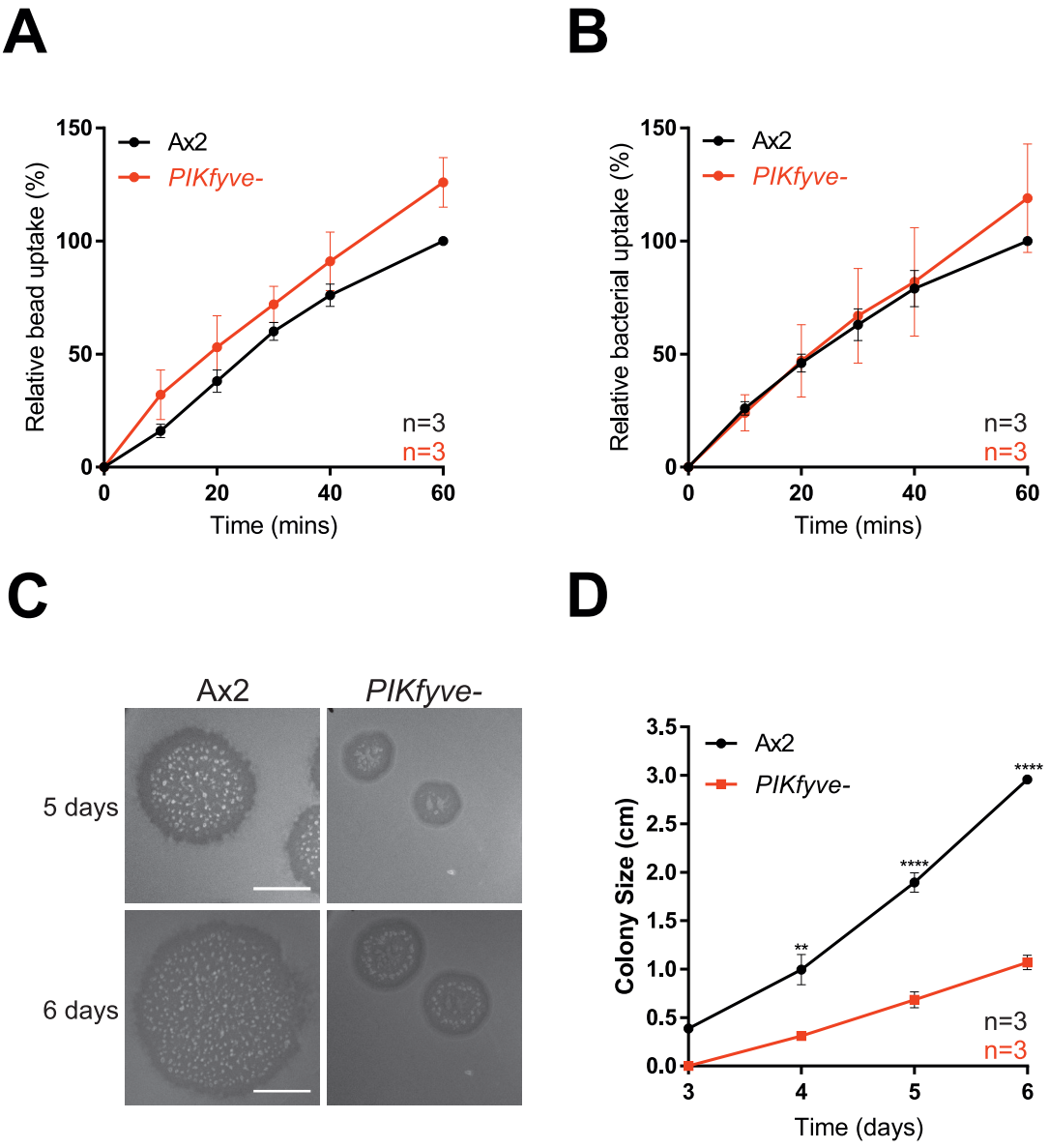


**Supplementary figure 3: *PIKfyve-* in Ax2 genetic background is comparable to knockout in Ax3**

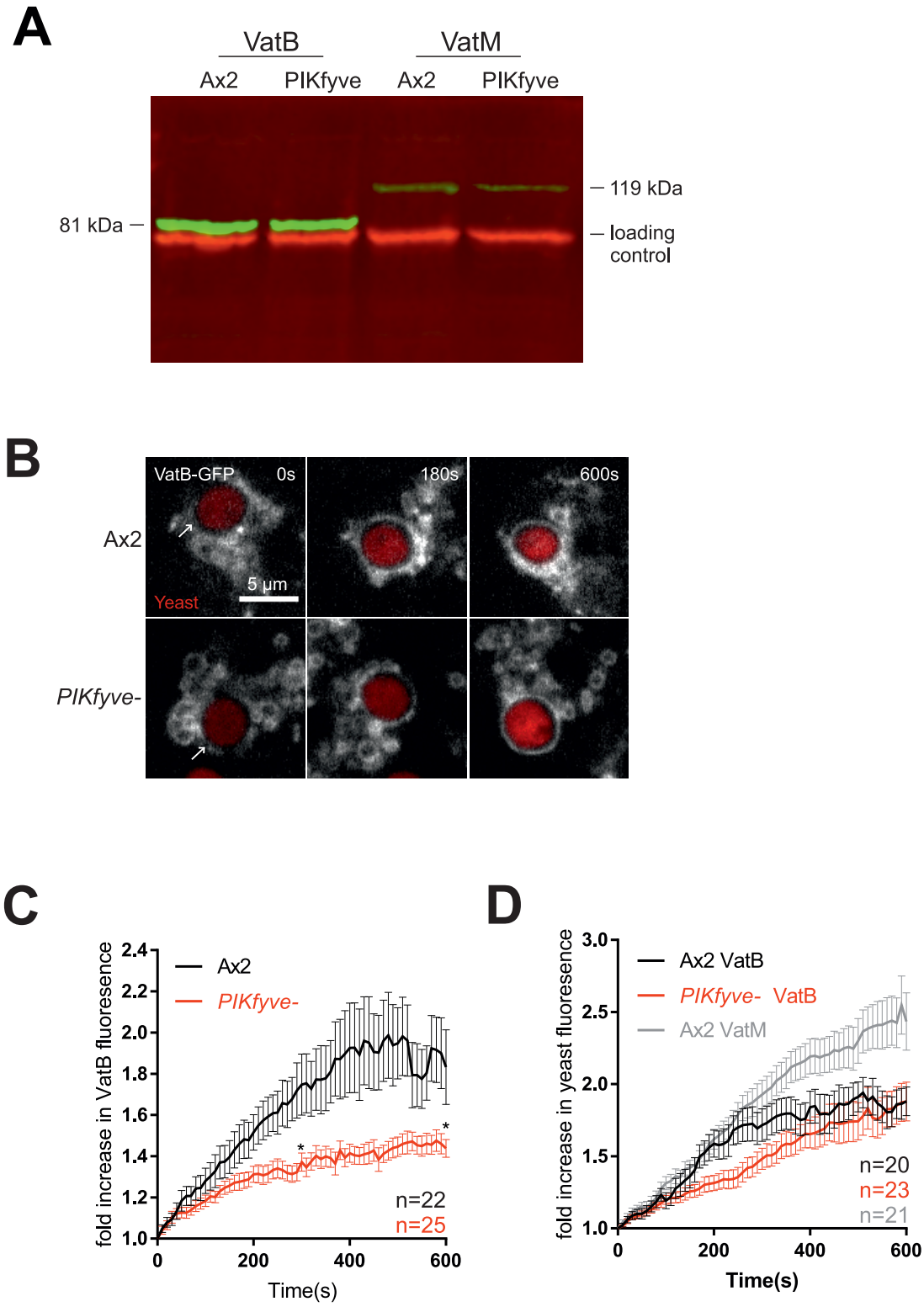


# Supplementary figure 4: VatB expression has a dominant negative effect on acidification